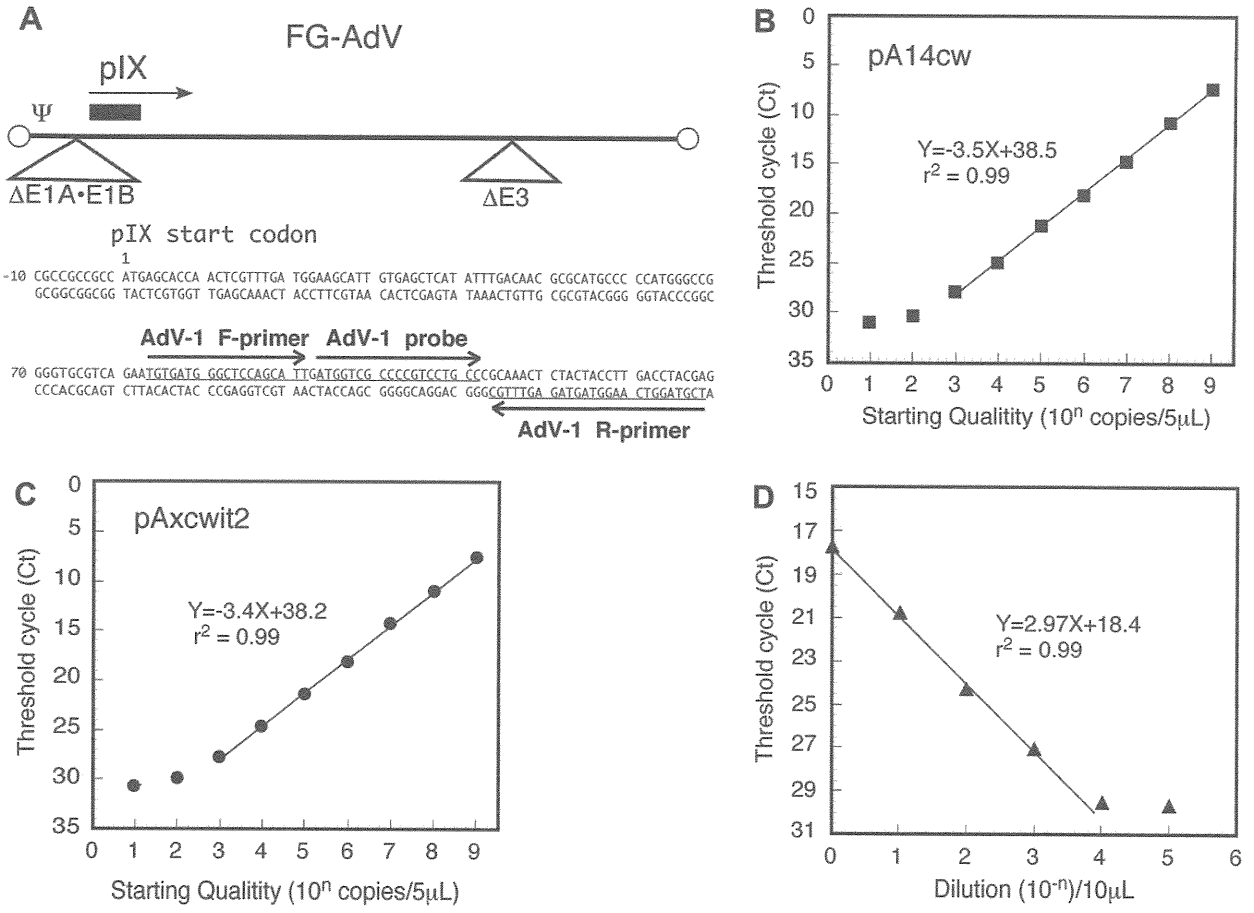

Fig. 2. (A) Position of the AdV-1 primers and the fluorogenic probe. The locations of the packaging signal (Ψ) and the coding region of the pIX gene are indicated. The arrows indicate the direction of transcription. AdV-1 F-primer, R-primer, and probe were designed using the program Primer Express 1.5 (Applied Biosystems), and their sequences are underlined. The primers and probes were selected according to the manufacturer's guidelines. The fluorogenic probes contained FAM (6-carboxylfluoroescein) at the 5′-end and TAMRA (6-carboxyltetramethylrhodamine) at the 3′-end. This set of primers/probe recognizes the coding region of the pIX gene. (B), (C), and (D) are the standard calibration curves for plasmids, cosmids and FG-AdV including the pIX gene, respectively. The standard calibration curves for the threshold cycle values (Ct) versus the copy number using serial dilutions of pA14cw (B) or pAxcwit2 (C) are shown. Similarly, serial dilutions of AxCAGFP vectors were used to generate the standard curve (D). The coefficients of correlation (r^2) are indicated.

of HeLa cells, respectively (column "GIT ratio", 0.3 for CV-1 and 0.06 for NIH-3T3), showing that GIT varied among different cell types.

However, because the control virus infected in parallel was identically influenced by the infection conditions, including the cell concentration and the cell type, the copy numbers of testing virus relative to that of the control virus can be calculated using the Ct value of the control virus as shown below. The relative GIT, called the rVT, is defined as follows:

$$\text{rVT} = (\text{control virus GIT}) \times 2^{(\text{control viral Ct} - \text{testing viral Ct})} (/\text{mL})$$

(Note that, because one *lower* Ct value means 2-fold *more* DNA, "$2^{(\text{testing viral Ct} - \text{control viral Ct})}$" is not correct).

For example, if control virus GIT, control viral Ct and testing viral Ct are 2.4×10^8 (copies/mL), 22.6 and 19.4, respectively, in a particular titration using CV-1 cells, the $\text{rVT} = 2.4 \times 10^8 \times 2^{(22.6-19.4)} = 2.4 \times 10^8 \times 2^{3.2} = 2.2 \times 10^9$ (copies/mL).

Because the rVTs of CV-1 and HeLa cells at the concentrations of 6.0×10^5 cells per well (full-sheet condition) were similar, i.e., 2.3×10^9 (copies/mL), the rVT calculated using the data of Fig. 2D can be applied to the rVT of HeLa cells. The rVTs measured using HeLa cell concentrations of 0.6×10^5, 2.0×10^5 and 6.0×10^5 cells per well were 0.9×10^9, 1.0×10^9 and 2.3×10^9 copies/μL, respectively (Table 1, rVT/mL): the ratio of rVTs obtained using three different cell concentrations (column "rVT ratio") was 0.4:0.4:1. Similar experiments using CV-1 cells indicated that the ratio was 1.2:1.2:1, showing that the rVT was less influenced by the cell concentration than the GIT. Table 1 also showed that, though the GIT of NIH-3T3 was extremely different from that of HeLa and CV-1, the rVT of NIH-3T3 was very similar to those of CV-1 and HeLa (column of "rVT ratio"). Therefore, even using different cell lines and dilutions, the rVT did not fluctuate, indicating that about the same rVT can be obtained using various types of cells other than HeLa cells for the purpose of titration. Because HeLa cells are commonly used worldwide, we recommend the use of HeLa cells for rVT measurements. Importantly, the present results also showed that the

Table 1
Differences between GIT and rVT among various cell concentration and cell lines.

Cells	No. of cells $\times 10^5$	GIT		rVT	
		Copies/mL $\times 10^9$	Ratio	rVT/mL $\times 10^9$	Ratio
HeLa	0.6	137.8 ± 6.4	4.9	0.9 ± 0.4	0.4
	2.0	89.5 ± 2.0	3.2	1.0 ± 0.2	0.4
	6.0	28.2 ± 1.8	1	2.3 ± 0.1	1
CV-1	6.0	8.2 ± 1.7	0.3	2.3 ± 0.1	1.0
NIH3T3 6.0	6.0	1.7 ± 0.3	0.06	1.0 ± 0.4	0.4

Two independent experiments were performed using the virus dilutions of 10^1 and 10^2.

Table 2
Infection conditions.

Condition	GIT/mL ($\times 10^9$)	Ratio
Plate	0.8 ± 0.3	1
Suspension	0.8 ± 0.2	1.0

The presentations are the same as Table 1.

Table 3
Days after infections.

Day	GIT/mL ($\times 10^9$)	Ratio
1	2.5 ± 0.1	1.6
2	1.6 ± 0.1	1
3	1.6 ± 0.4	1.0

The presentations are the same as Table 1.

rVT can be compared even when different cell lines or amounts of AdV were used.

The quality of the control virus does not significantly influence on the rVT value as far as the same lot of the control virus is used. Therefore, a conventional virus can be used as the control virus without purification. If strict comparison between the rVTs measured in different laboratories is needed, the adenovirus type 5 reference material may be useful and is available from ATCC (VR-1516) [23]. If a gene product of the testing virus is extremely deleterious to the target cells, the infected cells possibly grow slowly and the ratio of the copy number of the viral genome against that of β-actin on the cell chromosome may increase. However, if this is the case, the obtained rVT values of 10^{-1} dilution (high dose) and 10^{-2} dilution (low dose) must differ significantly, because the latter should be less influenced than the former. We have not experienced these cases.

3.4. Examination of infection conditions

We also examined whether the transduction efficiency of AdV differs when the cells to be infected are attached to a plate (plating method) or present in suspension (suspension method). In the former method, a monolayer of cells on the plate was incubated with an aliquot of AxCAGFP stock for 1 h for 37 °C, with shaking every 15 min before adding the medium. In the latter method, cells detached by trypsin were mixed with the virus, incubated for 5 min at room temperature, mixed with medium, and transferred to a 6-well or 24-well plate. The results showed no significant differences between the two methods for two different virus dilutions (Table 2). Because the suspension method is very simple and quick, we used the suspension method thereafter. Next, we examined the detected copy numbers of the transduced viral genome on days 1, 2 and 3. After washing the cells with PBS (−) on each day, the total infected-cell DNA was extracted, and the amounts of AdV genome were measured using qPCR (Table 3). The detected AdV copy number on day 1 was higher than that on day 2, but those on day 2 and day 3 were equal, suggesting that the number had reached a plateau level. The results were consistent with those for the Southern blot experiments (Fig. 1B, 48 h and 72 h). Consequently, we adopted day 2 for the measurement of rVT. Therefore, for the rVT method the infection protocol is very simple, and titration results can be obtained in only 2 days. The use of the infection protocol is not limited to AdV titration, but can also be used for ordinary AdV infection experiments. The rVT protocol is described in Supplementary Information.

3.5. Examples where the $TCID_{50}$ titer differed from the rVT

The ratio of the rVT value and the authentic $TCID_{50}$ titer were well correlated. AxEFLNLG is one example of an FG AdV; this AdV expresses neo protein unless the neo gene flanked by a pair of *lox*Ps is excised during Cre-mediated recombination. Because the neo gene is popularly used to establish neo-resistant cell lines, it must not be toxic. The rVT/mL and $TCID_{50}$/mL of a viral stock of this AdV were measured using CV-1 cells as a target and 293 cells, in which AdV proliferates, respectively. As shown in Table 4, in the first line, the ratio of rVT/$TCID_{50}$ was 0.3 using CV-1 for rVT; if HeLa cells are used for the rVT, the ratio should be $0.3 \times 0.6 \approx 0.2$ based on the data in Table 1. Thus, the $TCID_{50}$/mL was normally five times higher than the rVT/mL value when using HeLa as the target cells. Therefore, the ratio is normally useful when converting the values from one to another.

Table 4
Differences between rVT and $TCID_{50}$.

AdVs	rVT/mL	$TCID_{50}$/mL	rVT/$TCID_{50}$	Ratio
AxEFLNLG	$0.4 \pm 0.1 \times 10^9$	$1.8 \pm 0.2 \pm 10^9$	0.2	1
AxEFdsRed	$2.3 \pm 0.1 \times 10^9$	$0.3 \pm 0.1 \pm 10^9$	7.7	34.5
AxCANCre	$2.6 \pm 0.4 \times 10^7$	$3.1 \pm 0.9 \pm 10^7$	0.8	3.8

The presentations are the same as Table 1.

However, the ratio sometimes differed; for AxEFdsRed, an AdV that highly expresses dsRed protein, the copy number transduced to the target cells obtained using rVT was 18-times higher than that obtained using the $TCID_{50}$ method. AxCANCre, which highly expresses Cre recombinase, also produced an rVT value that was 3.3-times higher than that obtained using the $TCID_{50}$ method. Because the rVT value reflects the copy numbers in transduced target cells that are important for expression experiments, it is more valuable than the $TCID_{50}$ titer. Also, the rVT method can be applied for the titration of viruses that cannot proliferate in 293 cells, such as HD-AdV and other DNA and RNA viral vectors that do not replicate in the target cells.

In summary, we used Cre recombination and showed that the majority of the AdV genome detected in infected cells indicated successfully transduced molecules and that qPCR can certainly be used for AdV titration. Although cell concentrations and cell types influence the GIT tremendously, these factors can be corrected using a "control AdV" in parallel; hence, we established the rVT method, which can be used to determine the amount of actively infectious AdV genome present in the target cells. This method is quick, reliable, and superior to current titration methods using 293 cells.

Acknowledgments

The authors thank Ms. M. Terashima and Mr. Y. Ohno for technical support. Funding for this research was provided by a Grant in Aid for Scientific Research on Priority Areas from Ministry of Education, Culture, Sports, Science and Technology, Japan (to I.S.).

Appendix A. Supplementary data

Supplementary data associated with this article can be found, in the online version, at doi:10.1016/j.bbrc.2011.12.016.

References

[1] S. Kondo, Y. Takata, M. Nakano, I. Saito, Y. Kanegae, Activities of various FLP recombinases expressed by adenovirus vectors in mammalian cells, J. Mol. Biol. 390 (2009) 221–230.

[2] F.L. Graham, A.J. van der Eb, A new technique for the assay of infectivity of human adenovirus 5 DNA, Virology 52 (1973) 456–467.

[3] B. Precious, W.C. Russell, Growth, purification and titration of adenovirus, in: B.M. Mahy (Ed.), Virology: A Practical Approach, IRL Press, Oxford, 1985, pp. 193–205.
[4] Y. Kanegae, M. Makimura, I. Saito, A simple and efficient method for purification of infectious recombinant adenovirus, Jpn. J. Med. Sci. Biol. 47 (1994) 157–166.
[5] R. Mentel, E. Matthes, M. Janta-Lipinski, U. Wegner, Fluorescent focus reduction assay for the screening of antiadenoviral agents, J. Virol. Methods 59 (1996) 99–104.
[6] L. Philipson, Adenovirus assay by the fluorescent cell-counting procedure, Virology 15 (1961) 263–268.
[7] B. Bewig, W.E. Schmidt, Accelerated titering of adenoviruses, Biotechniques 28 (2000) 870–873.
[8] N. Mittereder, K.L. March, B.C. Trapnell, Evaluation of the concentration and bioactivity of adenovirus vectors for gene therapy, J. Virol. 70 (1996) 7498–7509.
[9] L. Ma, H.A. Bluyssen, M. De Raeymaeker, V. Laurysens, N. van der Beek, H. Pavliska, A.J. van Zonneveld, P. Tomme, H.H. van Es, Rapid determination of adenoviral vector titers by quantitative real-time PCR, J. Virol. Methods 93 (2001) 181–188.
[10] J. Crettaz, C. Olague, A. Vales, I. Aurrekoetxea, P. Berraondo, I. Otano, S. Kochanek, J. Prieto, G. Gonzalez-Aseguinolaza, Characterization of high-capacity adenovirus production by the quantitative real-time polymerase chain reaction: a comparative study of different titration methods, J. Gene Med. 10 (2008) 1092–1101.
[11] M. Puntel, J.F. Curtin, J.M. Zirger, A.K. Muhammad, W. Xiong, C. Liu, J. Hu, K.M. Kroeger, P. Czer, S. Sciascia, S. Mondkar, P.R. Lowenstein, M.G. Castro, Quantification of high-capacity helper-dependent adenoviral vector genomes in vitro and in vivo, using quantitative TaqMan real-time polymerase chain reaction, Hum. Gene Ther. 17 (2006) 531–544.
[12] F. Kreppel, V. Biermann, S. Kochanek, G. Schiedner, A DNA-based method to assay total and infectious particle contents and helper virus contamination in high-capacity adenoviral vector preparations, Hum. Gene Ther. 13 (2002) 1151–1156.
[13] V. Sandig, R. Youil, A.J. Bett, L.L. Franlin, M. Oshima, D. Maione, F. Wang, M.L. Metzker, R. Savino, C.T. Caskey, Optimization of the helper-dependent adenovirus system for production and potency in vivo, Proc. Natl. Acad. Sci. USA 97 (2000) 1002–1007.
[14] F.L. Graham, J. Smiley, W.C. Russell, R. Nairn, Characteristics of a human cell line transformed by DNA from human adenovirus type 5, J. Gen. Virol. 36 (1977) 59–74.
[15] Y. Kanegae, G. Lee, Y. Sato, M. Tanaka, M. Nakai, T. Sakaki, S. Sugano, I. Saito, Efficient gene activation in mammalian cells by using recombinant adenovirus expressing site-specific Cre recombinase, Nucleic Acids Res. 23 (1995) 3816–3821.
[16] Y. Kanegae, M. Terashima, S. Kondo, H. Fukuda, A. Maekawa, Z. Pei, I. Saito, High-level expression by tissue/cancer-specific promoter with strict specificity using a single-adenoviral vector, Nucleic Acids Res. 39 (2010) e7.
[17] S. Miyake, M. Makimura, Y. Kanegae, S. Harada, Y. Sato, K. Takamori, C. Tokuda, I. Saito, Efficient generation of recombinant adenoviruses using adenovirus DNA-terminal protein complex and a cosmid bearing the full-length virus genome, Proc. Natl. Acad. Sci. USA 93 (1996) 1320–1324.
[18] I. Saito, Y. Oya, K. Yamamoto, T. Yuasa, H. Shimojo, Construction of nondefective adenovirus type 5 bearing a 2.8-kilobase hepatitis B virus DNA near the right end of its genome, J. Virol. 54 (1985) 711–719.
[19] I. Saito, R. Groves, E. Giulotto, M. Rolfe, G.R. Stark, Evolution and stability of chromosomal DNA coamplified with the CAD gene, Mol. Cell Biol. 9 (1989) 2445–2452.
[20] J. Sambrook, D.W. Russell, Molecular Cloning, third ed., Cold Spring Harbor Laboratory Press, New York, 2001.
[21] M. Nakano, K. Odaka, Y. Takahashi, M. Ishimura, I. Saito, Y. Kanegae, Production of viral vectors using recombinase-mediated cassette exchange, Nucleic Acids Res. 33 (2005) e76.
[22] H. Fukuda, M. Terashima, M. Koshikawa, Y. Kanegae, I. Saito, Possible mechanism of adenovirus generation from a cloned viral genome tagged with nucleotides at its ends, Microbiol. Immunol. 50 (2006) 643–654.
[23] B. Huchins, N. Sajjadi, S. Seaver, A. Shepherd, S.R. Bauer, S. Simek, K. Carson, E. Aguilar-Cordova, Working toward an adenoviral vector testing standard, Mol. Ther. 2 (2000) 532–534.

Virus Research 160 (2011) 89–97

Contents lists available at ScienceDirect

Virus Research

journal homepage: www.elsevier.com/locate/virusres

Conditional gene expression in hepatitis C virus transgenic mice without induction of severe liver injury using a non-inflammatory Cre-expressing adenovirus

Tomoko Chiyo[a], Satoshi Sekiguchi[a], Masahiro Hayashi[a], Yoshimi Tobita[a], Yumi Kanegae[b], Izumu Saito[b], Michinori Kohara[a,*]

[a] Department of Microbiology and Cell Biology, The Tokyo Metropolitan Institute of Medical Science, 1-6, Kamikitazawa 2-chome, Setagaya-ku, Tokyo 156-8505, Japan
[b] Laboratory of Molecular Genetics, Institute of Medical Science, The University of Tokyo, Tokyo 108-8639, Japan

ARTICLE INFO

Article history:
Received 29 December 2010
Received in revised form 19 May 2011
Accepted 20 May 2011
Available online 30 May 2011

Keywords:
HCV transgenic mouse
Cre/loxP system
Recombinant adenovirus vector
EF1α promoter
Hepatitis

ABSTRACT

We previously established inducible-hepatitis C virus (HCV) transgenic mice, which expressed the HCV gene (nucleotides 294–3435) encoding the core, E1, E2, and NS2 proteins. The expression of these proteins is regulated by the Cre/loxP system and an adenovirus vector (AdV) that expresses Cre DNA recombinase (Cre) controlled by the CAG promoter (AxCANCre). Recent studies have demonstrated that AxCANCre injection alone results in severe liver injury by induction of the adenovirus protein IX (Ad-pIX) gene. As a result, HCV protein expression in transgenic mice livers was only short-term. In contrast, the EF1α promoter-bearing AdV induces slight Ad-pIX gene expression without inducing severe liver injury. Therefore, in the present study, we developed a Cre-expressing AdV that bears the EF1α promoter (AxEFCre) to express HCV protein in the transgenic mouse livers. In the non-transgenic mice injected with AxCANCre, alanine aminotransferase (ALT) levels were elevated and severe liver inflammation occurred; this was not observed in AxEFCre-injected mice. In contrast, AxEFCre-injected HCV transgenic mice showed milder liver inflammatory responses that were clearly due to HCV protein expression. Moreover, the AxEFCre injection enabled the transgenic mice to persistently express HCV protein. These results indicate that use of AxEFCre efficiently promotes Cre-mediated DNA recombination *in vivo* without a severe hepatitis response to AdV. This inducible-HCV transgenic mouse model using AxEFCre should be useful for research on HCV pathogenesis.

1. Introduction

Infection with the hepatitis C virus (HCV) is a major global health problem, as persistent viral infection leads to liver cirrhosis and hepatocellular carcinoma (Goodman and Ishak, 1995; Shepard et al., 2005). The chimpanzee is the only validated animal model for *in vivo* studies of HCV infection, while *in vivo* studies on the pathogenesis of HCV have been conducted using new animal models (Kremsdorf and Brezillon, 2007). Several groups have established transgenic mice that constitutively express single or multiple HCV protein(s) in the liver (Lerat et al., 2002; Moriya et al., 1997). However, in these mice, HCV protein expression begins *in utero*; as a result, they develop immune tolerance to the HCV antigens, and HCV-specific cellular responses or liver inflammation cannot be induced. To overcome these obstacles, we previously developed immunocompetent HCV transgenic mice in which HCV protein expression was tightly regulated by the Cre/*lox*P system (Wakita et al., 1998).

The E1- and E3-deleted adenovirus vector (AdV) has been widely used for both basic studies of gene function and for gene therapy *in vivo*. To deliver the *Cre* gene into the livers of HCV transgenic mice, we used an AdV that carries the CAG promoter linked to a nuclear localization signal-tagged Cre (AxCANCre), which has been used for Cre-mediated DNA recombination (Baba et al., 2005; Kobayashi et al., 2000; Shintani et al., 1999; Wakita et al., 1998). While AdV is relatively efficient in inducing transgene expression, several studies have shown that the viral vector itself can induce strong inflammatory responses in murine livers (Kafri et al., 1998; Wakita et al., 2000). Moreover, expression of transgenes via AdVs persists for only 2–4 weeks due to elimination of infected cells through immune responses directed against the AdVs (Akagi et al., 1997; Bangari and Mittal, 2006; Kafri et al., 1998; Sun et al., 2005; Wakita et al., 2000). To address these problems, the viral

* Corresponding author. Tel.: +81 3 5316 3232; fax: +81 3 5316 3137.
E-mail addresses: chiyo-tm@ncnp.go.jp (T. Chiyo), sekiguchi-st@igakuken.or.jp (S. Sekiguchi), mahayashi-kyt@umin.ac.jp (M. Hayashi), tobita-ys@igakuken.or.jp (Y. Tobita), kanegae@ims.u-tokyo.ac.jp (Y. Kanegae), isaito@ims.u-tokyo.ac.jp (I. Saito), kohara-mc@igakuken.or.jp (M. Kohara).

0168-1702/$ – see front matter © 2011 Elsevier B.V. All rights reserved.
doi:10.1016/j.virusres.2011.05.019

genes that cause cellular immune responses have been investigated. Recently, Nakai et al. (2007) reported that co-expression of adenovirus protein IX (Ad-pIX) resulted in AdV-induced immune responses. However, AdVs that carried the EF1α promoter did not induce Ad-pIX or increase the alanine aminotransferase (ALT) level, facilitating long-term transgene expression in mice.

In the present study, we generated a Cre-expressing AdV bearing the EF1α promoter (AxEFCre) to enable the persistent expression of HCV protein in the livers of inducible-HCV transgenic mice regulated by the Cre/*lox*P recombination system. When this AdV was used to express Cre in the HCV transgenic mouse livers, it induced less severe inflammatory responses and improved the long-term expression of HCV proteins compared to CAG promoter-bearing AdVs. Thus, AxEFCre efficiently promotes Cre-mediated DNA recombination *in vivo* without a severe hepatitis response to AdV and should be useful for HCV gene expression in the HCV transgenic mice.

2. Materials and methods

2.1. Cells

The 293 cells [CRL-1573, a human embryonic kidney cell line that contains the Ad5 E1 region; American Type Culture Collection (ATCC)] and HepG2 cells (HB-8065, a human hepatocellular carcinoma cell line; ATCC) were maintained in Dulbecco's modified Eagle's medium (DMEM; Nissui Pharmaceutical) supplemented with 10% fetal bovine serum (FBS; JRH Biosciences), 100 U/mL penicillin, and 100 μg/mL streptomycin (GIBCO) (10% FBS-DMEM). In addition, HepG2 cells containing the Cre reporter unit CALNLZ (Baba et al., 2005), termed Hep-CALNLZ cells, were selected for resistance to G418 (300 μg/mL; Sigma) and cultured in 10% FBS-DMEM.

2.2. Adenovirus vectors

E1- and E3-deleted AdVs derived from human adenovirus type 5 encoding expression units with a leftward orientation were used in this study. As expression units, untagged Cre or NLS-tagged Cre under the control of the CAG promoter (AxCANCre or AxCACre), untagged Cre or NLS-tagged Cre under the control of the EF1α promoter (AxEFNCre or AxEFCre), and untagged β-galactosidase (LacZ) under the control of the EF1α promoter (AxEFLacZ) were constructed (Fig. 1A). AxCANCre and AxCACre were generated as described previously (Kanegae et al., 1995). AxEFNCre, AxEFCre, and AxEFLacZ were constructed using pAxEFwtit2 DNA/RE Treatment (Nippon Gene). All of the AdVs were purified using two rounds of CsCl gradient centrifugation, and the titers of the concentrated and purified virus stocks were determined as described previously (Kanegae et al., 1994).

2.3. Animal procedures

HCV transgenic mice CN2-29 (C57BL/6 background) and normal C57BL/6 mice were used in the experiments. The CN2-29 transgenic mice express HCV genotype 1b proteins (core, E1, E2, and NS2 proteins) under the regulation of the Cre/*lox*P conditional switching system (Wakita et al., 1998). The transgenic mice were intravenously injected with each AdV at a dose of 1.0×10^9 plaque-forming units (PFU), and sacrificed 0.5, 7, or 21 days after injection for liver histology and biochemical analysis. All mice were bred in a pathogen-free facility and tested routinely for mouse hepatitis virus and other pathogens. All experiments using mice were approved by The Tokyo Metropolitan Institute of Medical Science Animal Experiment Committee and were performed in accordance with the animal experimentation guidelines of The Tokyo Metropolitan Institute of Medical Science.

2.4. Western blot detection of Cre and Ad-pIX

The HepG2 cells were placed in collagen-coated, 12-well plates and infected with the AdVs at a multiplicity of infection (MOI) of 20 or 100 for Western blot detection of Cre or Ad-pIX, respectively. After 24 h, the cells were washed with phosphate-buffered saline (PBS) and resolved in radioimmunoprecipitation assay (RIPA) buffer [10 mM Tris–HCl (pH 7.5), 0.15 M NaCl, 1% sodium dodecyl sulfate (SDS), 0.5% Nonidet P-40, protease inhibitor cocktail (Complete; Roche Molecular Biochemicals)]. The protein concentrations of the cell lysates were measured using the DC protein assay (Bio-Rad Laboratories). The cell lysates were electrophoresed on SDS–polyacrylamide gel, transferred to polyvinylidene difluoride membrane (GE Healthcare) activated with methanol, and blocked with 5% skim milk in PBS containing 0.1% Tween-20 (PBST). After washing with PBST, the membrane was incubated overnight at 4 °C in the presence of anti-Cre rabbit polyclonal antibody or anti-Ad-pIX rabbit polyclonal antibody (Nakai et al., 2007) prepared from hyper-immune rabbit sera, or anti-β-actin mouse monoclonal antibody (Sigma), followed by incubation with horseradish peroxidase (HRP)-conjugated $F(ab')_2$ of anti-rabbit or mouse IgG (GE Healthcare) for 1 h at room temperature. The expression levels of these proteins were visualized using the ECL system (GE Healthcare) and an LAS3000 imager (Fujifilm).

2.5. LacZ gene activation and cytotoxicity of Cre-expressing AdVs

The Hep-CALNLZ cells were cultured on collagen-coated, 96-well plates and infected with AdVs at various MOIs in four-fold serial dilutions. After 48 h, cytotoxicity assays were performed using the Cell Counting Kit-8 (Dojindo Molecular Technologies), according to the manufacturer's instructions. To detect *LacZ* expression, the cells were fixed with 4% paraformaldehyde in PBS for 10 min, washed with PBS, and incubated in X-Gal solution (5 mM potassium ferricyanide, 5 mM potassium ferrocyanide, and 2 mM $MgCl_2$ in PBS) containing 0.5 mg/mL 5-bromo-4-chloro-3-indolyl-β-D-galactopyranoside (X-Gal; WAKO Pure Chemicals) at 37 °C overnight.

2.6. Extraction of total RNA and quantification of Ad-pIX mRNA levels

The HepG2 cells were infected with the AdVs at an MOI of 100 and were harvested after 24 h. The CN2-29 transgenic mice were injected with the AdVs at a dose of 1.0×10^9 PFU and were sacrificed to obtain their liver samples after 12 h. Total RNA was extracted from the cells or mouse livers using the RNeasy Mini Kit (Qiagen) and RNase-free DNase (Qiagen). Reverse transcription was performed using the High Capacity cDNA Reverse Transcription Kit (Applied Biosystems). Copy numbers of the Ad-pIX cDNA were assessed by quantitative real-time detection polymerase chain reaction (RTD-PCR) with the specific probe AdIX-354-S25FT (5′-[FAM]-TCAGCAGCTGTTGGATCTGCGCCAC-[TAMRA]-3′); AdIX-327-S24 (5′-TTTGACCCGGGAACTTAATGTCGT-3′) and AdIX-387-R19 (5′-GGAGGAAGCCTTCAGGGCA-3′) were used as primers. The standard curve was generated using pAxEFLacZ. Analyses were conducted using an ABI PRISM 7700 Sequence Detection System with TaqMan Universal PCR Master Mix (Applied Biosystems).

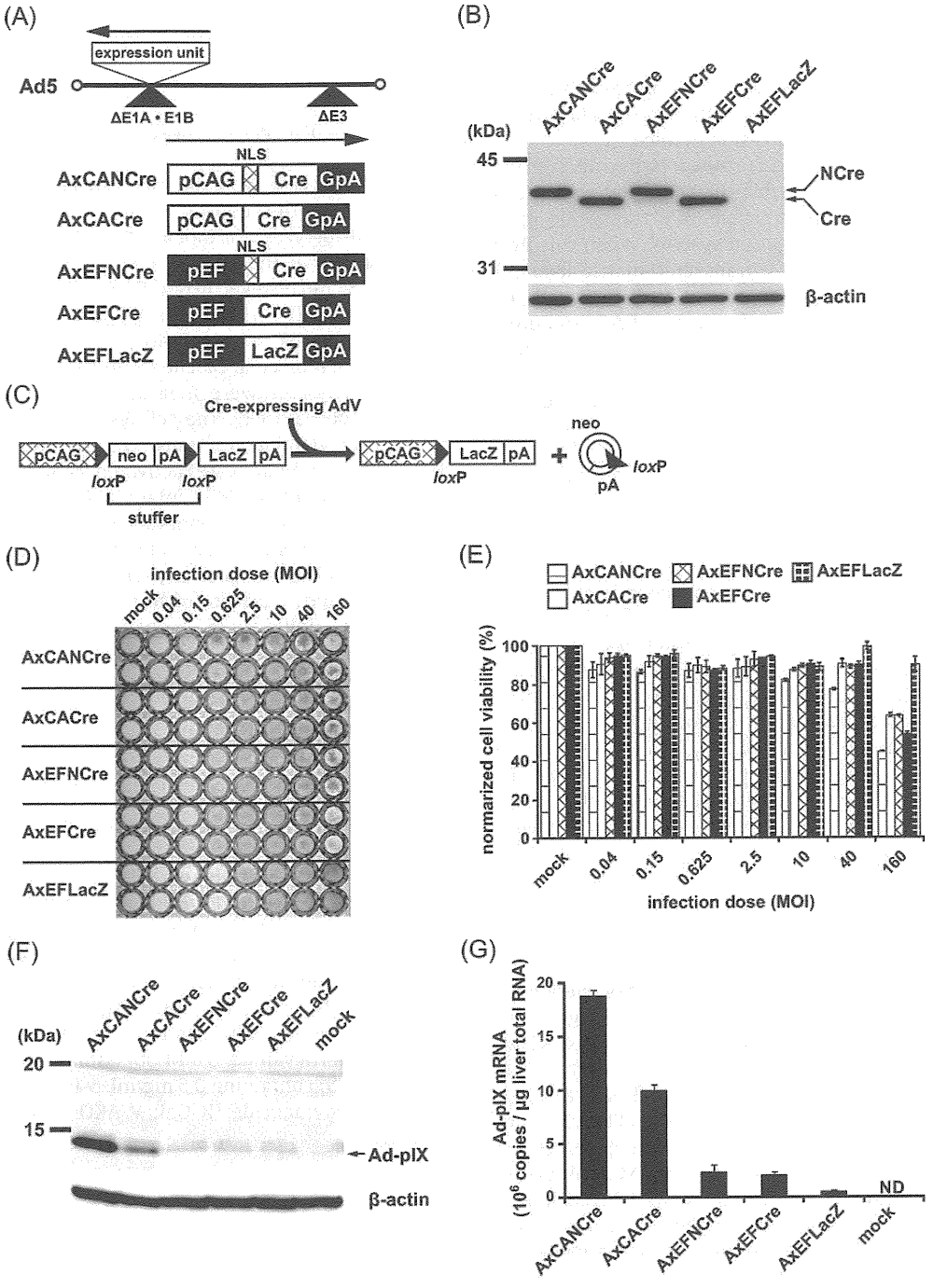

Fig. 1. Generation of AdVs expressing Cre under the control of different promoters. pCAG, CAG promoter; pEF, EF1α promoter; GpA, rabbit β-globin poly(A) signal; NLS, nuclear localization signal; neo, neomycin-resistance gene; pA, poly(A) signal; LacZ, β-galactosidase; Ad-pIX, adenovirus protein IX. (A) Structures of Cre-expressing AdVs. NLS-tagged Cre (NCre) or Cre were expressed under the control of the CAG or EF1α promoter. AxEFLacZ, which expresses LacZ under the control of the EF1α promoter, was used as a control. (B) Cre protein expression. HepG2 cells were infected with AdVs at an MOI of 20. After 24 h, total protein extracts from the cells were subjected to Western blotting. The detected β-actin protein is also shown. Note that mobility is slightly reduced when Cre is tagged with NLS (lanes, AxCANCre and AxEFNCre). (C) Schematic representation of *LacZ* transgene activation mediated by Cre-expressing AdV in Hep-CALNLZ cell chromosomes. Cre recognizes a pair of its target sequences *lox*P and removes the stuffer region as a circular DNA, resulting in expression of the transgene by the CAG promoter. (D) Cre recombination activity. Hep-CALNLZ cells were infected with Cre-expressing AdVs at the indicated dosages (four-fold serial dilutions; MOI range, 0.04–160). After 48 h, the cells were fixed and stained using X-gal staining. The first lane contains the mock-infected controls. The AxEFLacZ-infected lanes show the *LacZ*-gene-expressed control. (E) Cre cytotoxicities. Hep-CALNLZ cells were infected with AdVs at the indicated dosages (four-fold serial dilutions; MOI range, 0.04–160). After 48 h, cell viability was measured using a Cell Counting Kit-8. (F) Ad-pIX protein expression. HepG2 cells were infected with AdVs at an MOI of 100. After 24 h, total protein extracts from the cells were subjected to Western blotting. The detected β-actin protein is also shown. (G) mRNA expression of Ad-pIX. HepG2 cells were infected with AdVs at an MOI of 100. After 24 h, total RNA extracts from the cells were subjected to reverse transcription and quantitative RTD-PCR with an Ad-pIX-specific probe and a primer pair. ND, not detected.

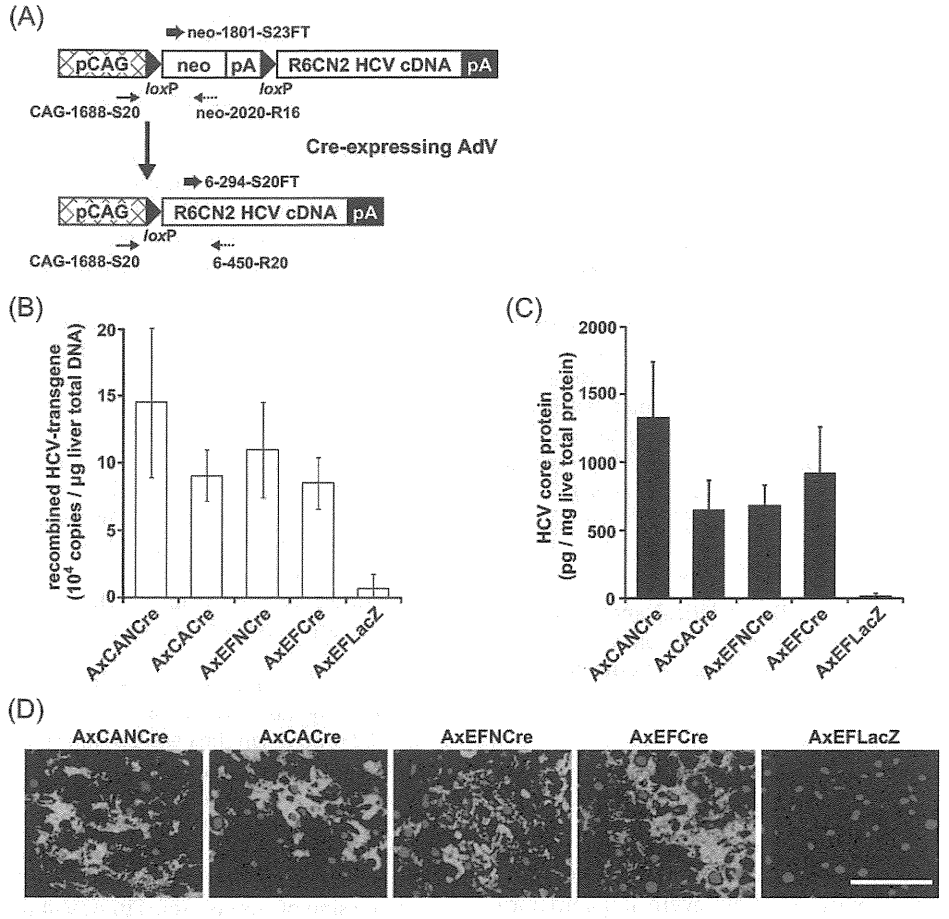

Fig. 2. Cre-mediated genomic DNA recombination and HCV core protein expression in transgenic mouse livers. (A) Structure of the Cre-mediated activation transgene unit CALNCN2 (Wakita et al., 1998). pCAG, CAG promoter; neo, neomycin-resistance gene; pA, poly(A) signal. The R6CN2 HCV cDNA (nucleotides 294–3435) contains the core, E1, E2, and NS2 regions. This construct does not allow HCV mRNA transcription prior to Cre-mediated DNA recombination, detected with the primer pair CAG-1688-S20 and neo-2020-R16. When Cre-expressing AdV is injected, the *neo* gene and poly(A) signal are removed by recombination between two *lox*P sequences. The recombined HCV transgene is detected with the primer pair CAG-1688-S20 and 6-450-R20. (B) Determination of Cre-mediated DNA recombination. CN2-29 transgenic mice were injected with 1.0×10^9 PFU for each AdV, and liver samples were harvested 7 days post-injection. Genomic DNA was extracted from the livers, and the numbers of copies of the recombined HCV-transgenes were determined using quantitative RTD-PCR with specific probes (6-294-S20FT) and a primer pair (CAG-1688-S20 and 6-450-R20). The values shown are means ± S.D. of more than three individual specimens. (C) Measurements of HCV core protein concentration in liver samples obtained from CN2-29 transgenic mice 7 days after injection of 1.0×10^9 PFU for each AdV. The samples were homogenized and the concentrations of HCV core protein were determined by EIA. The values shown are means ± S.D. of three individual specimens. (D) Immunofluorescence analysis of HCV core proteins. Liver sections of CN2-29 transgenic mice 7 days after injection of 1.0×10^9 PFU for each AdV were fixed and co-stained with rabbit anti-core polyclonal antibody (green) and DAPI (blue). Scale bar, 50 μm.

2.7. Determination of Cre-mediated HCV transgene recombination in mouse livers

The transgenic mouse livers were digested at 37 °C overnight in lysis buffer [50 mM Tris–HCl (pH 8.0), 0.1 M NaCl, 20 mM EDTA, 1% SDS] containing 1 mg/mL proteinase K. Total genomic DNA was then extracted using the phenol–chloroform extraction method. The copy numbers of the recombined HCV transgene in the livers were assessed via quantitative RTD-PCR (Takeuchi et al., 1999) with the specific probe 6-294-S20FT (5′-[FAM]-TGATAGGGTGCTTGCGAGTG-[TAMRA]-3′) and the primer pair CAG-1688-S20 (5′-GGTTGTTGTGCTGTCTCATC-3′) and 6-450-R20 (5′-ACAGGTAAACTCCACCAACG-3′) (Fig. 2A). The standard curve was generated using pCALNCN2/59-2 (Wakita et al., 1998) and quantitative RTD-PCR with the specific probe neo-1801-S23FT (5′-[FAM]-TCAAGAGACAGGATGAGGATCGT-[TAMRA]-3′) and the primer pair CAG-1688-S20 (5′-GGTTGTTGTGCTGTCTCATC-3′) and neo-2020-R16 (5′-TGCCTCGTCCTGCAGT-3′) (Fig. 2A). The *GAPDH* gene was used as an internal control for all samples. Analyses were carried out on an ABI PRISM 7700 Sequence Detection System with TaqMan Universal PCR Master Mix (Applied Biosystems).

2.8. Quantitation of HCV core proteins in mouse liver lysates

The transgenic mouse livers were homogenized in 0.5 mL RIPA buffer, and centrifuged at 15,000 rpm for 10 min at 4 °C. The protein concentrations of the supernatants were measured using the Bradford method (DC protein assay; Bio-Rad). The concentrations of HCV core proteins in the liver samples were determined using the Ortho HCV core protein ELISA kit (Eiken Chemical).

2.9. Biochemical analyses of mouse sera

Sequential blood samples were obtained by orbital bleeding after each AdV administration, and the sera were isolated by centrifugation at 10,000 rpm for 3 min at 4 °C. Serum ALT levels were determined using the Transaminase-CII Test A (Wako Pure Chemicals).

2.10. Histology and immunohistochemical staining

The liver samples were fixed with 4% paraformaldehyde in PBS, paraffin-embedded, sectioned at 4-μm thickness, and stained

with hematoxylin and eosin (H&E). Liver histology was evaluated according to modified Histology Activity Index (HAI) scores in three categories: piecemeal necrosis, spotty necrosis, and portal inflammation (Knodell et al., 1981; Yang et al., 1994).

The liver tissues were frozen in OCT compound (Tissue Tech) for immunohistochemical staining of HCV core proteins. The sections were fixed with a 1:1 solution of acetone:methanol at −20 °C for 10 min and then washed with PBS. Subsequently, the sections were incubated with the IgG fraction of an anti-HCV core rabbit polyclonal antibody (RR8) (Wakita et al., 1998) labeled with biotin in blocking buffer for 1 h at 4 °C. The sections were incubated with strept–avidin-conjugated horseradish peroxidase for 30 min at room temperature. Immunohistochemical staining was conducted using the Tyramide Signal Amplification Kit (Molecular Probes). Fluorescently labeled sections were stained with 4′,6-diamidino-2-phenylindole (DAPI; Molecular Probes) to stain the cell nuclei at room temperature before cover slipping. Fluorescence was observed under a fluorescence microscope (Carl Zeiss).

2.11. Statistical analysis

Data are shown as the mean ± S.D. Statistical analyses were performed using analysis of variance (ANOVA) followed by the Student–Newman–Keuls (SNK) test or analyzed using the unpaired Student's *t*-test. Statistical significance was established at $p < 0.05$.

3. Results

3.1. Generation of Cre-expressing AdVs

To enable HCV transgenic mice using the Cre/*lox*P system to express HCV protein persistently without severe inflammatory responses to AdV, we first constructed AdVs that expressed Cre with or without a nuclear localization signal (NLS) tag (AxEFNCre or AxEFCre, respectively) together with *LacZ* under the control of the EF1α promoter (AxEFLacZ) (Fig. 1A). AxCANCre and AxCACre were also generated to compare the impacts of using the CAG promoter and the EF1α promoter (Fig. 1A). Expression of Cre proteins from various AdVs was confirmed in human liver-derived HepG2 cells by Western blot analysis (Fig. 1B). Cre protein expression levels were not significantly different whether the gene was expressed under the control of the CAG or the EF1α promoter in the HepG2 cells (Fig. 1B). Next, we examined the recombination activities of Cre expressed via the AdVs using the Hep-CALNLZ cell line, HepG2 cells that express CALNLZ (Fig. 1C). When the Cre-expressing AdVs bearing the CAG or EF1α promoters infected these cells, the blue color produced by *LacZ* activation was observed for MOIs of 0.15–160. The cells infected with AxEFLacZ showed the blue staining in an MOI-dependent manner (Fig. 1D, lane AxEFLacZ). In contrast, the color faded for MOIs >40 when the Cre-expressing AdVs were used (Fig. 1D, lanes AxCANCre, AxCACre, AxEFNCre, and AxEFCre). At an MOI of 160, all of the Cre-expressing AdVs resulted in cytotoxicity, while the LacZ-expressing AdV did not affect cell viability (Fig. 1E).

AdV-induced immune responses are partly caused by co-expression of Ad-pIX (Nakai et al., 2007). To confirm the protein expression levels of Ad-pIX due to the AdVs, we performed Western blotting with anti-Ad-pIX sera (Fig. 1F). When HepG2 cells were infected with AdVs bearing the CAG promoter, significant amounts of Ad-pIX were detected as 14-kDa bands (Fig. 1F, lanes AxCANCre and AxCACre). In contrast, when using AdVs bearing the EF1α promoter, the 14-kDa band representing Ad-pIX was undetectable, as was the case for mock-infected HepG2 cells (Fig. 1F, lanes AxEFNCre, AxEFCre, AxEFLacZ, and mock). We also examined the mRNA expression levels of Ad-pIX and obtained similar results that correlated with the protein expression levels (Fig. 1G).

3.2. HCV gene expression and core protein production mediated by various Cre-expressing AdVs in transgenic mouse livers

The HCV transgenic mouse CN2-29 contains a reporter unit (CALNCN2) that is activated by Cre and conditionally expresses the HCV gene (Fig. 2A; Wakita et al., 1998). To assess the efficiency of Cre-expressing AdVs in promoting HCV gene expression, we intravenously injected the CN2-29 transgenic mice with various AdVs. At 7 days post-injection, Cre protein expression was confirmed by Western blot analysis of liver lysates (data not shown). The recombined HCV transgene levels in the livers were determined by quantitative RTD-PCR using specific probes and primer pairs, as described in Section 2 (Fig. 2A and B). When each Cre-expressing AdV was injected, the respective recombined HCV transgene was detectable; AxCANCre-injected CN2-29 transgenic mice expressed the highest levels of the recombined HCV transgene in their livers (Fig. 2B). CN2-29 transgenic mice injected with AdVs expressing NLS-tagged Cre had higher levels of the recombined HCV transgene in their livers (Fig. 2B, AxCANCre and AxEFNCre). This result suggests that NLS-tagged Cre efficiently translocated to the cell nucleus, which is consistent with our previous data (Baba et al., 2005). However, the levels of the recombined HCV transgene were not correlated with the expression level of HCV core protein (Fig. 2C).

The core protein levels in the livers were measured by enzyme immunoassay (EIA) as described in Section 2. The expression of the E1 and E2 proteins in the CN2–29 transgenic mouse livers has been shown previously (Wakita et al., 1998). The mean core protein level was 1.3 ng/mg total protein in the CN2-29 transgenic mouse livers 7 days after administration of AxCANCre (Fig. 2C). AxCACre- and AxEFNCre-injected mice expressed approximately one-half of the core protein levels resulting from AxCANCre injection (Fig. 2C).

Expression of core proteins in AdV-injected CN2-29 transgenic mouse livers was confirmed through immunofluorescence staining. Core proteins were expressed in the hepatocytes in the lobules of liver sections from Cre-expressing AdV-injected mice (Fig. 2D). In contrast, AxEFLacZ-injected transgenic mice did not express core proteins (Fig. 2C and D).

3.3. Liver injury and Ad-pIX expression in HCV transgenic mice injected with AdVs

To evaluate hepatocellular injury caused by expression of HCV proteins in CN2-29 transgenic mice injected with Cre-expressing AdVs, we serially estimated the serum ALT levels (Fig. 3A). For AxCANCre, the serum ALT level was elevated on day 5 and peaked 1–2 weeks post-injection (Fig. 3A, open triangle). ALT levels in AxCACre-injected transgenic mice were also elevated, although these levels declined over time (Fig. 3A, open circle). When AxEFNCre or AxEFCre was injected, ALT levels did not immediately increase, although they gradually increased after day 5 (Fig. 3A, closed triangle and closed circle, respectively). Injection of AxEFLacZ did not increase serum ALT levels in the CN2-29 transgenic mice (Fig. 3A, closed rectangle).

We also performed histological analyses of liver sections from CN2–29 transgenic mice 7 days after AdV injection (Fig. 3B). We found that severe inflammation with lymphocyte infiltration and spotty necrosis were diffusely observed in the livers of mice injected with the AdVs bearing the CAG promoter (AxCACre and AxCANCre) (Fig. 3B, a,b). In contrast, AxEFNCre-injected and AxEFCre-injected transgenic mouse livers exhibited mild inflammation without massive piecemeal necrosis on day 7 (Fig. 3B, c,d). No inflammation was observed in the AxEFLacZ-injected mice (Fig. 3B, e).

To confirm the expression levels of Ad-pIX in AdV-injected transgenic mice, we determined Ad-pIX mRNA in the liver using

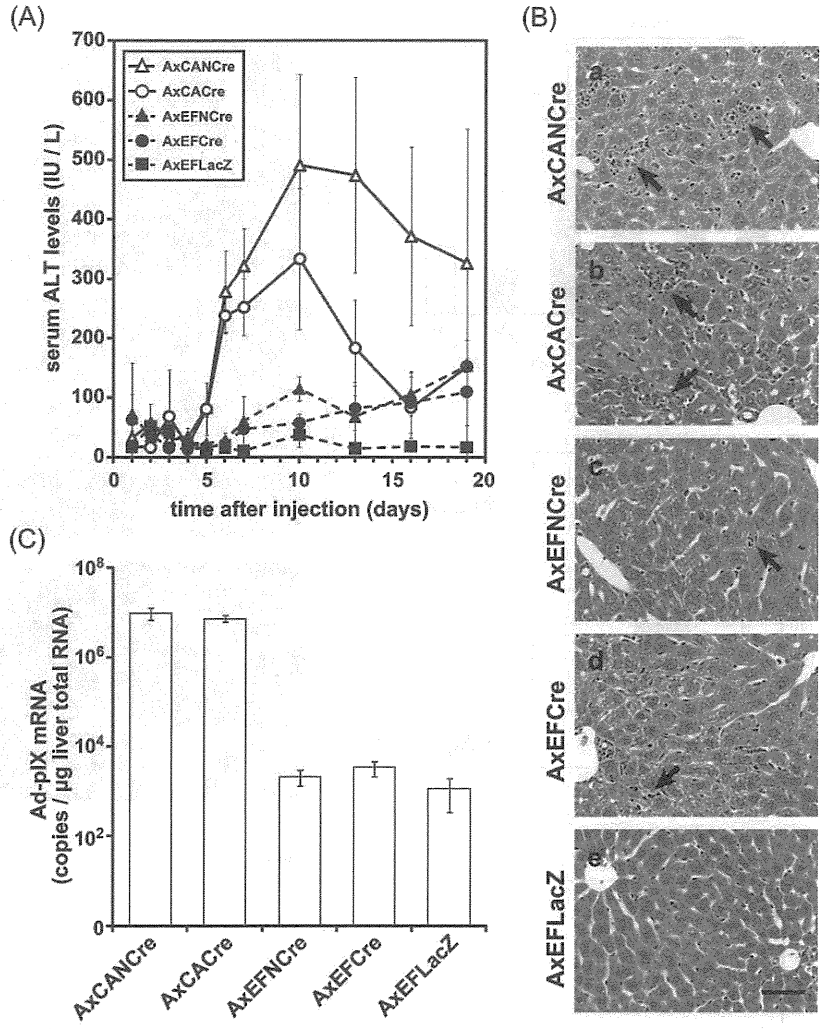

Fig. 3. Effects of AdVs on liver injuries in HCV transgenic mice. (A) Serum ALT levels were measured at the indicated time-points in CN2-29 transgenic mice injected with 1.0×10^9 PFU AxCANCre (open triangle), AxCACre (open circle), AxEFNCre (closed triangle), AxEFCre (closed circle), and AxEFLacZ (closed rectangle). The ALT levels are shown as means ± S.D. of three individual specimens. (B) Histopathologic changes in the livers of transgenic mice 7 days after injection of each AdV. The liver sections were stained with H&E. The arrows represent lymphocyte infiltrations. Scale bar, 50 μm. (C) mRNA expression of Ad-pIX in the livers. CN2-29 transgenic mice were injected with 1.0×10^9 PFU of the AdVs. After 12 h, the livers were harvested. The total RNA extracts from the livers were subjected to reverse transcription and RTD-PCR with an Ad-pIX-specific probe and a primer pair, as described in Section 2. The numbers of copies of Ad-pIX mRNA are shown as means ± S.D. of three individual specimens.

reverse transcription and quantitative RTD-PCR, as described under Section 2. The copy numbers of Ad-pIX mRNA were quite high in transgenic mice that were injected with AdV bearing the CAG promoter (Fig. 3C). The observed inflammation levels were consistent with the expression levels of Ad-pIX.

3.4. *Liver inflammatory responses to the HCV protein inducibly expressed by AdVs in transgenic mice*

Because our results indicated that severe liver injuries were caused by AdVs bearing the CAG promoter, we evaluated liver inflammatory responses to the HCV protein inducibly expressed by AdVs in transgenic mice 7 days post-injection according to the modified HAI scoring system (Fig. 4A) (Knodell et al., 1981; Yang et al., 1994). Among the transgenic mice, more severe liver damage was observed in those that were injected with Cre-expressing AdVs bearing the CAG promoter (Fig. 4A, AxCANCre and AxCACre) compared to those injected with Cre-expressing AdVs bearing the EF1α promoter (Fig. 4A, AxEFNCre and AxEFCre).

Because AxEFCre more efficiently expressed HCV proteins than AxEFNCre (Fig. 2C and D), we injected AxEFCre into transgenic mice and wild-type mice to examine the effects of HCV protein expression. The severity of liver inflammation in the AxEFCre-injected transgenic mice was significantly greater than in the AxEFCre-injected wild-type mice or the AxEFLacZ-injected transgenic mice (Fig. 4A and B).

Seven days after AdV administration, serum ALT levels of AxCANCre-injected wild-type mice were significantly higher than those of AxEFCre-injected wild-type mice (Fig. 4C). This ALT elevation was observed in both transgenic and wild-type mice injected with AxCANCre (Fig. 4C). In contrast, AxEFCre was injected into the two groups, transgenic mice expressing HCV proteins exhibited more severe liver injury than wild-type mice (Fig. 4C and D).

3.5. *Effects of Cre-expressing AdV bearing the EF1α promoter on HCV protein expression in transgenic mouse livers*

To investigate whether CN2-29 transgenic mice injected with AdVs bearing the EF1α promoter showed liver inflammation caused

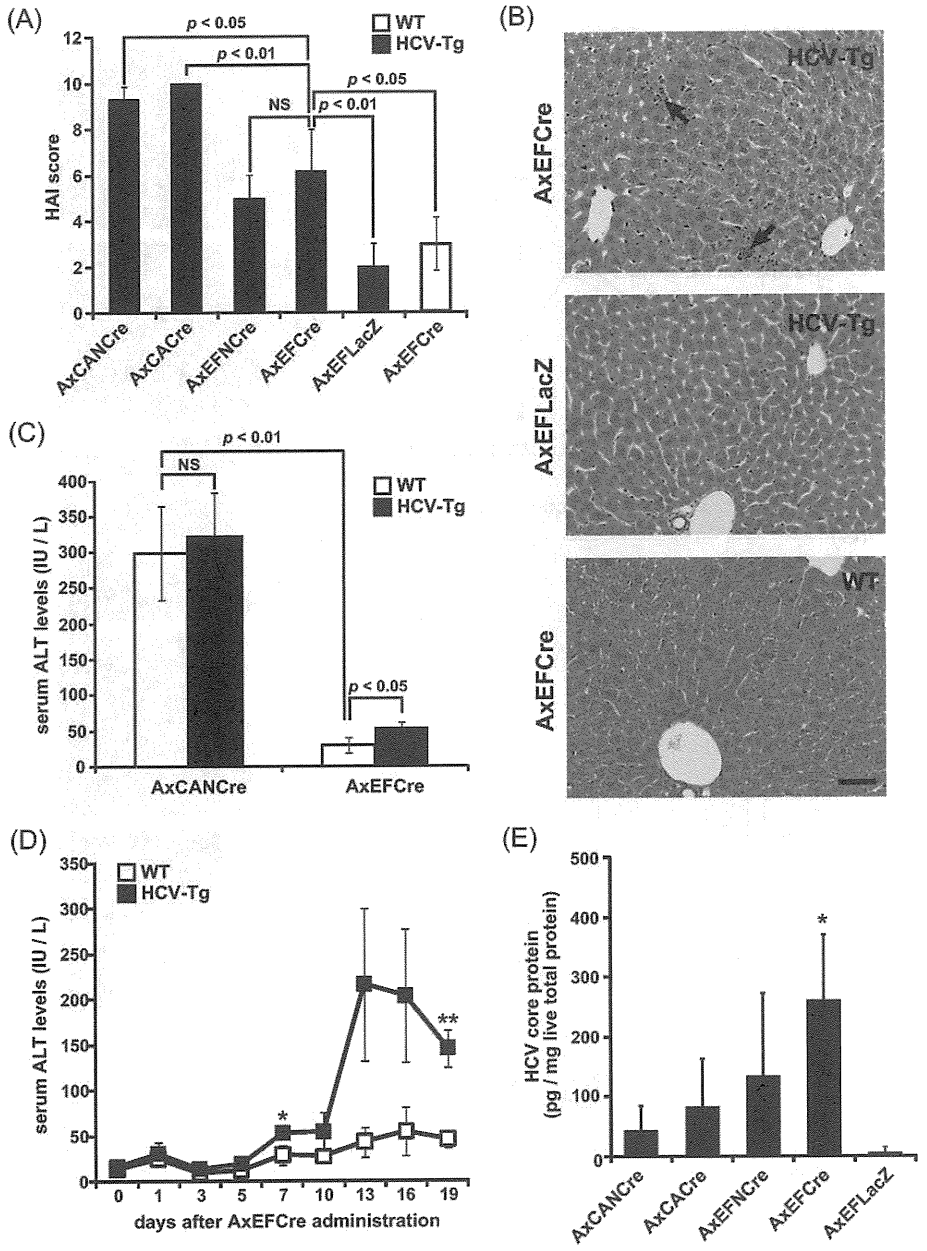

Fig. 4. Liver inflammatory responses due to HCV protein expression induced by AxEFCre. (A) Histopathology of mouse livers after injection of AdVs. Histopathologic features of the livers of CN2-29 transgenic mice (HCV-Tg, closed bars) injected with 1.0×10^9 PFU of AxCANCre, AxCACre, AxEFNCre, AxEFCre, or AxEFLacZ, and wild-type mice that were injected with 1.0×10^9 PFU of AxEFCre at day 7 post-injection (WT, opened bar). Pathologic changes were evaluated by light microscopy of H&E-stained sections of the mouse livers using the modified HAI scoring system. The extent of pathology was scored on a scale from 0 (none) to 12 (severe). All of the scores are means ± S.D. of more than three individual specimens. Statistical analysis was performed using an unpaired Student's *t*-test. NS, not significant. (B) Histopathologic changes resulting from HCV protein expression in mouse livers. CN2-29 transgenic mice (HCV-Tg) were injected with AxEFCre or AxEFLacZ and wild-type mice (WT) were injected with AxEFCre 7 days post-injection. The liver sections were stained with H&E. The arrows represent piecemeal necrosis. Scale bars, 50 μm. (C) Serum ALT levels with or without HCV protein expression 7 days after administration of the AdVs. Statistical analysis was performed using an unpaired Student's *t*-test between CN2-29 transgenic mice (HCV-Tg) and wild-type mice (WT). NS, not significant. (D) Sequential changes in serum ALT levels after AxEFCre administration. Serum ALT levels were measured at the indicated time-points in CN2-29 transgenic mice (HCV-Tg, closed square) or wild-type mice (WT, opened square) that were injected with 1.0×10^9 PFU AxEFCre. ALT levels are shown as means ± S.D. of more than three individual specimens. Statistical analysis was performed using an unpaired Student's *t*-test between CN2-29 transgenic mice (HCV-Tg) and wild-type mice (WT). $^*p < 0.05$; $^{**}p < 0.01$. (E) HCV core protein expression 21 days after AdV administration in transgenic mouse livers. CN2-29 transgenic mice were injected with 1.0×10^9 PFU for each AdV. After 21 days, the livers were harvested and homogenized. The concentrations of HCV core proteins in liver lysates were determined by EIA. The values shown are means ± S.D. of three individual experiments. Statistical analysis was performed using an ANOVA, followed by the SNK test. $^*p < 0.05$.

by persistently expressed HCV proteins, we evaluated core proteins by EIA in transgenic mouse livers 21 days post-injection of the AdVs (Fig. 4E). HCV core protein expression was scarcely detectable in the transgenic mice injected with AxCANCre, while the AxEFCre-injected transgenic mice showed significantly higher levels of core protein expression (Fig. 4E). Although, the AxCANCre injection was scarcely observed at day 21 in the transgenic mice (Fig. 4E), HCV core protein expression induced by AxEFCre injection was observed until at least day 56.

4. Discussion

In the present study, we demonstrated that Cre-expressing AdVs bearing the EF1α promoter induce HCV gene expression and

HCV protein production without induction of severe liver injury in inducible-HCV transgenic mice. We further observed that increases in serum ALT levels and liver inflammation were related to HCV protein expression mediated by AxEFCre injection. Moreover, AxEFCre injection enabled the transgenic mice to persistently express HCV proteins.

In previous studies, HCV transgenic mice constitutively expressing HCV proteins exhibited symptoms of steatosis and/or hepatocellular carcinoma, but did not show inflammatory or immunopathologic changes (Lerat et al., 2002; Moriya et al., 1997, 1998; Sun et al., 2001). Inducible-HCV transgenic mouse lineages, in which HCV protein expression is regulated, have enabled investigation of the immunopathogenesis of HCV protein expression. HCV transgenic mice regulated by the Cre/*lox*P system (Sun et al., 2005; Tumurbaatar et al., 2007; Wakita et al., 1998) or the tetracycline regulatory system (Ernst et al., 2007) exhibit inducible and liver-specific expression of HCV proteins. Inducible-HCV transgenic mice using the Cre/*lox*P system with an AdV that expresses Cre under the control of the CAG promoter (AxCANCre) exhibit HCV-specific immune responses (Wakita et al., 1998, 2000). The inducible-HCV CN2-29 transgenic mice, which express the core, E1, E2, and NS2 proteins, have HCV-specific cytotoxic T lymphocytes (Takaku et al., 2003; Wakita et al., 1998, 2000).

However, they show severe inflammatory responses to AxCANCre itself and thus, HCV protein expression is only transient (Wakita et al., 2000). These significant obstacles have limited the utility of inducible-HCV transgenic mice. Therefore, to deliver the *Cre* gene into the liver, non-adenoviral induction methods have been developed (Ho et al., 2008; Sun et al., 2005; Zhu et al., 2006). Meanwhile, adenoviral genes that cause cellular immune responses have been identified and modified AdVs that do not trigger host immune responses have been developed (Palmer and Ng, 2005). A recent study demonstrated that immune responses to AdVs bearing the CAG promoter were associated with co-expression of Ad-pIX, whereas immune responses were minimal when transgene expression was controlled by the EF1α promoter (Nakai et al., 2007). Therefore, we postulated that severe inflammation of mouse livers after administration of Cre-expressing AdVs bearing the CAG promoter (AxCANCre) might be caused by expression of Ad-pIX. In the present study, we generated Cre-expressing AdVs bearing the EF1α promoter (AxEFCre) and infected HCV transgenic mice. AxEFCre-injected mice expressed much less Ad-pIX mRNA and did not show the increased levels of ALT or severe liver inflammation as did Cre-expressing AdVs under the control of the CAG promoter (Fig. 3). In contrast, AxCANCre administration caused severe liver injury in both HCV transgenic mice and wild-type mice (Fig. 4D; Wakita et al., 2000). AxEFCre administration caused liver injury in the HCV transgenic mice, but not in the wild-type mice (Fig. 4A–D). These results suggest that AxEFCre alone induces only minimal host immune responses compared to AxCANCre; therefore, the liver inflammatory responses exhibited by AxEFCre-injected transgenic mice were clearly due to expression of HCV proteins. Because AxCANCre injection alone causes severe liver injuries, most of the hepatocytes infected with AxCANCre are eliminated and HCV protein expression in the livers of transgenic mice is only transient (Wakita et al., 2000). On the other hand, AxEFCre injection did not induce such severe liver injuries. The AxEFCre-injected HCV transgenic mice showed milder liver inflammation in response to expression of HCV proteins and persistently expressed HCV proteins without elimination of hepatocytes infected with AxEFCre.

In conclusion, HCV gene expression mediated by the Cre/*lox*P system and a Cre-expressing AdV that bears the EF1α promoter, AxEFCre, enables Cre-mediated recombination of transgenes in mice without inducing severe liver injury due to the AdV itself. Moreover, this inducible-HCV transgenic mouse model should be useful for investigation of liver injury due to HCV and the pathogenesis of HCV.

Acknowledgments

The authors wish to thank Mitsugu Takahashi for breeding the transgenic mice. This study was supported by grants from the Ministry of Education, Culture, Sports, Science and Technology of Japan; the Program for Promotion of Fundamental Studies in Health Sciences of the Pharmaceuticals and Medical Devices Agency of Japan; and the Ministry of Health, Labor and Welfare of Japan.

References

Akagi, K., Sandig, V., Vooijs, M., Van der Valk, M., Giovannini, M., Strauss, M., Berns, A., 1997. Cre-mediated somatic site-specific recombination in mice. Nucleic Acids Res. 25 (9), 1766–1773.

Baba, Y., Nakano, M., Yamada, Y., Saito, I., Kanegae, Y., 2005. Practical range of effective dose for Cre recombinase-expressing recombinant adenovirus without cell toxicity in mammalian cells. Microbiol. Immunol. 49 (6), 559–570.

Bangari, D.S., Mittal, S.K., 2006. Current strategies and future directions for eluding adenoviral vector immunity. Curr. Gene Ther. 6 (2), 215–226.

Ernst, E., Schonig, K., Bugert, J.J., Blaker, H., Pfaff, E., Stremmel, W., Encke, J., 2007. Generation of inducible hepatitis C virus transgenic mouse lines. J. Med. Virol. 79 (8), 1103–1112.

Goodman, Z.D., Ishak, K.G., 1995. Histopathology of hepatitis C virus infection. Semin. Liver Dis. 15 (1), 70–81.

Ho, K.J., Bass, C.E., Kroemer, A.H., Ma, C., Terwilliger, E., Karp, S.J., 2008. Optimized adeno-associated virus 8 produces hepatocyte-specific Cre-mediated recombination without toxicity or affecting liver regeneration. Am. J. Physiol. Gastrointest. Liver Physiol. 295 (2), G412–G419.

Kafri, T., Morgan, D., Krahl, T., Sarvetnick, N., Sherman, L., Verma, I., 1998. Cellular immune response to adenoviral vector infected cells does not require de novo viral gene expression: implications for gene therapy. Proc. Natl. Acad. Sci. U S A 95 (19), 11377–11382.

Kanegae, Y., Lee, G., Sato, Y., Tanaka, M., Nakai, M., Sakaki, T., Sugano, S., Saito, I., 1995. Efficient gene activation in mammalian cells by using recombinant adenovirus expressing site-specific Cre recombinase. Nucleic Acids Res. 23 (19), 3816–3821.

Kanegae, Y., Makimura, M., Saito, I., 1994. A simple and efficient method for purification of infectious recombinant adenovirus. Jpn. J. Med. Sci. Biol. 47 (3), 157–166.

Knodell, R.G., Ishak, K.G., Black, W.C., Chen, T.S., Craig, R., Kaplowitz, N., Kiernan, T.W., Wollman, J., 1981. Formulation and application of a numerical scoring system for assessing histological activity in asymptomatic chronic active hepatitis. Hepatology 1 (5), 431–435.

Kobayashi, N., Fujiwara, T., Westerman, K.A., Inoue, Y., Sakaguchi, M., Noguchi, H., Miyazaki, M., Cai, J., Tanaka, N., Fox, I.J., Leboulch, P., 2000. Prevention of acute liver failure in rats with reversibly immortalized human hepatocytes. Science 287 (5456), 1258–1262.

Kremsdorf, D., Brezillon, N., 2007. New animal models for hepatitis C viral infection and pathogenesis studies. World J. Gastroenterol. 13 (17), 2427–2435.

Lerat, H., Honda, M., Beard, M.R., Loesch, K., Sun, J., Yang, Y., Okuda, M., Gosert, R., Xiao, S.Y., Weinman, S.A., Lemon, S.M., 2002. Steatosis and liver cancer in transgenic mice expressing the structural and nonstructural proteins of hepatitis C virus. Gastroenterology 122 (2), 352–365.

Moriya, K., Fujie, H., Shintani, Y., Yotsuyanagi, H., Tsutsumi, T., Ishibashi, K., Matsuura, Y., Kimura, S., Miyamura, T., Koike, K., 1998. The core protein of hepatitis C virus induces hepatocellular carcinoma in transgenic mice. Nat. Med. 4 (9), 1065–1067.

Moriya, K., Yotsuyanagi, H., Shintani, Y., Fujie, H., Ishibashi, K., Matsuura, Y., Miyamura, T., Koike, K., 1997. Hepatitis C virus core protein induces hepatic steatosis in transgenic mice. J. Gen. Virol. 78 (7), 1527–1531.

Nakai, M., Komiya, K., Murata, M., Kimura, T., Kanaoka, M., Kanegae, Y., Saito, I., 2007. Expression of pIX gene induced by transgene promoter: possible cause of host immune response in first-generation adenoviral vectors. Hum. Gene. Ther. 18 (10), 925–936.

Palmer, D.J., Ng, P., 2005. Helper-dependent adenoviral vectors for gene therapy. Hum. Gene. Ther. 16 (1), 1–16.

Shepard, C.W., Finelli, L., Alter, M.J., 2005. Global epidemiology of hepatitis C virus infection. Lancet Infect. Dis. 5 (9), 558–567.

Shintani, Y., Yotsuyanagi, H., Moriya, K., Fujie, H., Tsutsumi, T., Kanegae, Y., Kimura, S., Saito, I., Koike, K., 1999. Induction of apoptosis after switch-on of the hepatitis B virus X gene mediated by the Cre/loxP recombination system. J. Gen. Virol. 80 (12), 3257–3265.

Sun, J., Bodola, F., Fan, X., Irshad, H., Soong, L., Lemon, S.M., Chan, T.S., 2001. Hepatitis C virus core and envelope proteins do not suppress the host's ability to clear a hepatic viral infection. J. Virol. 75 (24), 11992–11998.

Sun, J., Tumurbaatar, B., Jia, J., Diao, H., Bodola, F., Lemon, S.M., Tang, W., Bowen, D.G., McCaughan, G.W., Bertolino, P., Chan, T.S., 2005. Parenchymal expression of CD86/B7.2 contributes to hepatitis C virus-related liver injury. J. Virol. 79 (16), 10730–10739.

Takaku, S., Nakagawa, Y., Shimizu, M., Norose, Y., Maruyama, I., Wakita, T., Takano, T., Kohara, M., Takahashi, H., 2003. Induction of hepatic injury by hepatitis C-virus-

specific CD8± murine cytotoxic T lymphocytes in transgenic mice expressing the viral structural genes. Biochem. Biophys. Res. Commun. 301, 330–337.
Takeuchi, T., Katsume, A., Tanaka, T., Abe, A., Inoue, K., Tsukiyama-Kohara, K., Kawaguchi, R., Tanaka, S., Kohara, M., 1999. Real-time detection system for quantification of hepatitis C virus genome. Gastroenterology 116 (3), 636–642.
Tumurbaatar, B., Sun, Y., Chan, T., Sun, J., 2007. Cre-estrogen receptor-mediated hepatitis C virus structural protein expression in mice. J. Virol. Methods 146 (1–2), 5–13.
Wakita, T., Katsume, A., Kato, J., Taya, C., Yonekawa, H., Kanegae, Y., Saito, I., Hayashi, Y., Koike, M., Miyamoto, M., Hiasa, Y., Kohara, M., 2000. Possible role of cytotoxic T cells in acute liver injury in hepatitis C virus cDNA transgenic mice mediated by Cre/loxP system. J. Med. Virol. 62 (3), 308–317.
Wakita, T., Taya, C., Katsume, A., Kato, J., Yonekawa, H., Kanegae, Y., Saito, I., Hayashi, Y., Koike, M., Kohara, M., 1998. Efficient conditional transgene expression in hepatitis C virus cDNA transgenic mice mediated by the Cre/loxP system. J. Biol. Chem. 273 (15), 9001–9006.
Yang, Y., Ertl, H.C., Wilson, J.M., 1994. MHC class I-restricted cytotoxic T lymphocytes to viral antigens destroy hepatocytes in mice infected with E1-deleted recombinant adenoviruses. Immunity 1 (5), 433–442.
Zhu, H.Z., Wang, W., Feng, D.M., Sai, Y., Xue, J.L., 2006. Conditional gene modification in mouse liver using hydrodynamic delivery of plasmid DNA encoding Cre recombinase. FEBS Lett. 580 (18), 4346–4352.

Published online 4 November 2010

Nucleic Acids Research, 2011, Vol. 39, No. 2 e7
doi:10.1093/nar/gkq966

High-level expression by tissue/cancer-specific promoter with strict specificity using a single-adenoviral vector

Yumi Kanegae*, Miho Terashima, Saki Kondo, Hiromitsu Fukuda, Aya Maekawa, Zheng Pei and Izumu Saito

Laboratory of Molecular Genetics, Institute of Medical Science, University of Tokyo, 4-6-1 Shirokanedai, Minato-ku, Tokyo 108-8639, Japan

Received March 26, 2010; Revised September 24, 2010; Accepted October 3, 2010

ABSTRACT

Tissue-/cancer-specific promoters for use in adenovirus vectors (AdVs) are valuable for elucidating specific gene functions and for use in gene therapy. However, low activity, non-specific expression and size limitations in the vector are always problems. Here, we developed a 'double-unit' AdV containing the Cre gene under the control of an α-fetoprotein promoter near the right end of its genome and bearing a compact 'excisional-expression' unit consisting of a target cDNA 'upstream' of a potent promoter between two *lox*Ps near the left end of its genome. When Cre was expressed, the expression unit was excised as a circular molecule and strongly expressed. Undesired leak expression of Cre during virus preparation was completely suppressed by a dominant-negative Cre and a short-hairpin RNA against Cre. Using this novel construct, a very strict specificity was maintained while achieving a 40- to 90-fold higher expression level, compared with that attainable using a direct specific promoter. Therefore, the 'double-unit' AdV enabled us to produce a tissue-/cancer-specific promoter in an AdV with a high expression level and strict specificity.

INTRODUCTION

Because tissue-specific promoters enable us to express a gene in a cell-type-specific manner *in vivo* or in a primary tissue culture, such promoters offer an attractive approach to studying the specific functions of a gene product in the tissues of experimental animals, such as in the brain where cells of different types are present together in the same region. The use of transgenic/knockout mice and adenovirus vectors (AdVs) are the most common approaches for utilizing these promoters. Among such promoters, those specific to malignant cells may be valuable for specific gene therapy or the diagnosis of cancer.

However, one drawback of such promoters is that their expression levels are much lower than those of a versatile promoter, such as the cytomegalovirus (CMV) immediate-early, CAG (1) or EF1α (2) promoters. For example, the α-fetoprotein (AFP) promoter, which is a relatively strong promoter among tissue-specific promoters, is reported to be ~500-fold less active than the CAG promoter (3), limiting its usefulness. Another important problem associated with the use of these promoters is that their specificity was often not sufficiently strict. One possible reason is that the excised segment of a specific promoter lacks the sufficient control of specific silencers and shows some 'basal level' of expression. In some cases, the lack of specificity might arise from the DNA elements surrounding the promoter, rather than the intrinsic character of the specific promoter (4,5). In human gene therapy using AdV, a strict specificity is critically important for safety as well as efficacy.

As one solution, we previously reported a 'double-infection' method (3), in which the virtual activity of AFP promoter was increased by about 50-fold while maintaining a strict specificity. With this method, two AdVs are infected simultaneously: one AdV contains a 'switch unit' consisting of Cre gene under the control of AFP promoter, and the other AdV bears a 'target unit' consisting of the CAG promoter,

*To whom correspondence should be addressed. Tel: +81 3 54495556; Fax: +81 3 5449 5432; Email: kanegae@ims.u-tokyo.ac.jp
Present addresses:
Saki Kondo, Cell Regulation Laboratory, Paterson Institute for Cancer Research, University of Manchester, Wilmslow Road, Manchester, M20 4BX, UK
Hiromitsu Fukuda, Japan Animal Referral Medical Center, 2-5-8 Kuji, Takatsu-ku, Kawasaki-shi, Kanawawa 213-0032, Japan

*lox*P, the stuffer sequence, second *lox*P, and a target cDNA, in that order. In non-hepatocarcinoma cells, the expression of the reporter cDNA remains turned off. However, in target hepatocarcinoma cells, AFP promoter in the switch unit of one AdV is turned on, leading to the production of Cre enzyme; this in turn leads to the excision of the stuffer sequence in the other AdV by Cre-mediated site-specific recombination, leaving the CAG promoter and the target gene connected only through a *lox*P sequence and enabling the strong expression of the target gene. Even when AFP promoter is weak and only a small quantity of Cre protein is produced, Cre can act as an enzyme multiple times, allowing most of the target AdV genomes to be processed eventually and accounting for the very high level of expression that can be obtained. The double infection method has been applied in numerous *in vivo* studies examining gene therapy for lung, colon and gastric cancers using the carcinoembryonic antigen promoter (6–10), for thyroid cancer using the thyroglobulin promoter (11), for hepatocellular carcinoma using AFP promoter (12), for prostate cancer using the prostate-specific antigen promoter (13) and for astrocytoma using the astrocytoma-specific promoter for GFAP (14). The method has also been applied in brain research using a modified, neuron-specific promoter of superior cervical ganglion 10 (15).

However, because the double-infection method uses two different AdVs simultaneously, controlling the infection is complicated and not often reproducible. Additionally, the toxicity and inflammation are at least doubled, compared with a single viral infection, for transducing the same amount of the target unit. Moreover, since a single cell infected with only one of the vectors does not produce any target protein, many such cells remain unused, causing a low expression as a result of dilution (12). Therefore, as a simpler, safer and more effective vector, an AdV bearing both the switch and the target unit simultaneously in a single genome is needed. However, the development of such an AdV has been regarded as being very difficult, since the sum of the lengths of both units exceeds the maximum length of the AdV genome. Furthermore, a leak in the expression of Cre can produce a large amount of stuffer-lacking AdV during vector preparation, causing severe non-specific expression. In addition, an enhancer of the potent promoter in the target unit may decrease the specificity of the specific promoter in the switch unit. Thus, a new vector is needed to solve these problems.

Here, we report the development and successful preparation of an AdV containing both units in a single genome. The vector, called a 'double-unit' AdV, possesses an extraordinary 'excisional-expression' structure and solves the aforementioned problems simultaneously, because the target unit of this vector lacks a stuffer sequence and because the target gene is expressed not from its genome, but from an excised circular DNA. The developed AdV shows a high level of expression (40- to 90-fold) while maintaining a very strict specificity.

MATERIALS AND METHODS

Cells and AdVs

The human embryo kidney cell line, 293 (16), constitutively expresses adenoviral E1 genes and supports the replication of E1-substituted AdV. HepG2 (17) and HuH7 (18) cells are human hepatocellular carcinoma cell lines that produce AFP. SK-Hep-1 (19) cells are a human hepatocellular carcinoma cell line that lack AFP production. HeLa cells, derived from cervical cancer, do not express AFP (20). The cell line CV1 is derived from African green monkey kidney. The AFP promoter used here was the (AB)2S6 AFP promoter (3). The EF1α promoter has been described previously (2). AxA2ANCre was described previously (3). AxLR14EL-AC, AxLR16EL-AC, AxLR16EFL, Ax-AC, AxNZ, AxLNZCAL, AxALNZCAL, AxA2AdsR and AxEFdsR are described for the first time in this work. AdVs described here were constructed using cosmid transfection (21). All the aforementioned viruses except for AxA2AdsR and AxEFdsR possessed E3 region with a 2.4-kb deletion, while the latter two viruses bore E3 region with the 1.9-kb deletion described in reference (21) (see 'Discussion' section). The switch unit was inserted at the *Sna*BI site (nt position 35 770), located 165-nt downstream from the right end of the adenovirus-5 (Ad5) genome. Because the standard Ad5 genome does not contain the *Sna*BI site, we generated a restriction site using nucleotide substitution, inserted a *Swa*I linker, and then cloned the switch unit. All the viruses were purified using a CsCl step gradient (22) and titrated using a method measuring 50% tissue culture infectious dose ($TCID_{50}$) (22); the viral particle: $TCID_{50}$ ratio was ~20:100, including double-unit viruses. The viral titer of all the AdV, including double-unit vectors was measured with $TCID_{50}$ using normal 293 cells.

Dominant negatives and shRNAs of Cre and isolation of Cre-suppressed 293 cells

dnCreRY was a dominant negative of Cre, where Arg173 and Tyr324 were mutated to Ala and Phe, respectively. pyCANCRYit2 is a plasmid expressing dnCreRY under the control of CAG promoter. The dnCreRY cDNA was excised as a *Sma*I-*Bgl*II fragment and inserted into pTrcHis2A (Invitrogen) between the *Ecl*36II and *Bgl*II sites under the *Escherichia coli* trc promoter (23). The *Bss*SI-*Sph*I fragment containing trc-dnCreRY was transferred upstream of the cos site of cosmid pAxLR16EL-AC and pAxLR14EL-AC, which were both derived from pAxcwit2 (21). The resulting cosmids were named ptdC-AxLR16EL-AC and ptdC-AxLR14EL-AC, respectively. shCreD (TA0493-4-D) was an shRNA of Cre, gatccGAAGCAACTCATCGATTGAtagtgctcctg gttgTCAATCGATGAGTTGCTTCtttttta (Cre sequences are in capitals), which efficiently suppressed Cre activity. TA0493-4-D was inserted under the human U6 promoter of plasmid pBAsi hU6 Pur (Takara Bio). The 293dnCreRY8 and 293shCreD13 were the best cell lines containing dnCreRY under the control of CAG promoter

and shCreD driven by human U6 promoter suppressing Cre activity among those tested, respectively.

To generate 293dnCreRY8, pBCANCRYSAPur was constructed, expressing dnCreRY under the control of the CAG promoter and the puromycin-resistant (Pur^R) gene under the control of the SV40 early promoter (Figure 5a). To generate 293shCreD13, pBSAPurhU6shCre was constructed, expressing one of the short-hairpin (sh) RNAs against Cre under the control of the human U6 promoter (Takara Bio) and the Pur^R gene identical to that expressed by pBCANCRYSAPur (Figure 5b). Ten micrograms of each plasmid DNA were transfected into 293 cells using Transfast^R (Promega). Two days after transfection, puromycin was added at a concentration of 2.5 μg/ml. We selected the cell line that most efficiently caused a reduction of Cre activity for the simultaneous transfection in Cre-expressing and target pCALNLG plasmids (24).

Preparation of total cell DNA for restriction-enzyme digestion and for real-time PCR

Infected cell DNA was prepared on a 24-well plate as previously described (25) with some modifications: the cells were suspended in 0.4 ml of TNE-PK [50 mM Tris–HCl (pH 8), 100mM NaCl, 10 mM EDTA, 100 mg/ml proteinase K], followed by the addition of SDS (final 0.1%). After incubation at 55°C for 2 h, the mixture was extracted once with phenol–chloroform and once with chloroform, and precipitated with 1 or 1.5 volumes of ethanol at −20°C for >1 h and then washed once with 70% ethanol. The pellet was dissolved with 50 ml of TE containing 20 mg/ml RNase A and stored at −20°C. This DNA was sufficient not only for real-time PCR but also for gel electrophoresis to observe the structure of the AdV genome.

To detect viral DNA, total DNA extracted from AxLR16EL-AC-infected, Cre-suppressed 293 cells in a 24-well plate was digested with *Bmg*BI. The *Bmg*BI recognition sequence, CACGTG, contains a -CG- dinucleotide, which is mostly methylated in the mammalian genome and cannot be cleaved by a restriction enzyme, while replicating adenoviral DNA is not methylated and can be cleaved. Consequently, restricted patterns of only adenoviral DNA can be seen.

Quantification of AdV transduction efficiency and expressed RNA

Total cell DNA was prepared as described above. Real-time PCR was performed to detect the adenovirus genome using a probe for the pIX gene, and human chromosome was simultaneously detected using a probe for the β-actin gene or the ornithine transcarbamylase (OTC) gene. The threshold cycle (cT) values were obtained. All the probes used in the study are shown in Table 1. The cT value of the AdV was corrected according to that for the human chromosome probe. The sequences of these probes were shown in Table 1. Infected cell RNA was prepared using the RNeasy protect mini kit (Qiagen) according to the manufacturer's protocol. To prepare the cDNA, the TaqMan Reverse Transcriptase Reagent kit (Applied BioSystems) was used. The sequences of the dsRed probes are shown in Table 1. The 18S rRNA primer used in the study were Ribosomal Eukaryotic 18S rRNA kit (Applied BioSystems).

Table 1. Sequences of probes used in real-time PCR

Probe[a]	Primer sequences[b]
AdV-1	F: TGTGATGGGCTCCAGCATT
	P: ATGGTCGCCCCGTCCTGCC
	R: TCGTAGGTCAAGGTAGTAGAGTTTGC
hOTC-1	F: CCACTACAAAATAAAGTGCAGCTGAA
	P: CCGTGACCTTCTCACTCTAAAAAACTT
	R: CTGATAGCCATAGCATATATTTAATTTCTTCTC
β-Act-1	F: CTCGCAGCTCACCATGGAT
	P: ATGATATCGCCGCGCTCGTCGT
	R: ATGCCGGAGCCGTTGTC
dsRed-1	F: GCAGCTGCCCGGCTACT
	P: CGTGGACTCCAAGCTGGACATCACCT
	R: CGATGGTGTAGTCCTCGTTGTG

18S rRNA primers used were Ribosomal Enkaryotic 18S rRNA kit (Applied BioSystems).
[a]Name of the probes. Reporters used were FAM except β-Act-1 (VIC reporter).
[b]F, forward primer; P, probe; R, reverse primer. Real-time PCR was purchased from Applied BioSystems.

To examine the expressed dsRed RNA, the cells were infected with AdV and total DNA and the total RNA was extracted. From the total DNA, the amounts of AdV genome and β-actin gene were simultaneously quantified using real-time PCR and the ratio of AdV genome per cell was obtained. Similarly, from the total RNA, the amounts of dsRed RNA and 18S-rRNA (the correction standard) were quantified using reverse transcription and real-time PCR, and the ratio of dsRed RNA to 18S-rRNA was obtained. Based on these results, the ratio of the dsRed RNA level between the two cell lines was calculated.

Detection of expressed fluorescence

To evaluate the different EF1α promoter versions, the cells were washed twice with Hank's balanced salt solution 3 days after transfection, and the intensity of GFP fluorescence was quantified using Fluoroskan Ascent FL (Labsystems) (26). Cells infected with AxLR16EL-AC and AxLR14EL-AC were sorted using dsRed fluorescence using FACS (FACSCalibur, Becton-Dikinson). The dsRed fluorescence was also measured using Ascent fluorescent meter. To calculate the relative strengths among the various promoters, the steady-state level of the expressed dsRed RNA together with the dsRed DNA in the AdV genome in infected cells was quantified using a real-time PCR (Prism 7000, Applied Biosystems), and the former value was divided by the latter.

RESULTS

Structure of 'double-unit' vector containing 'excisional-expression' unit

The structure of the 'double-unit' AdV vector AxLR16EL-AC is shown in Figure 1. This vector is a

first generation AdV containing the switch unit inserted near the right end of the adenovirus genome (27) (denoted in this paper at the E4 position) and the target unit inserted in the E1 region. Since the adenovirus genome can be packaged into a capsid up to ~105% of, or 2 kb more than, the wild-type genome size (28), it was impossible to generate an AdV containing both the switch and the target units using a typical construction strategy because of over-sizing. Therefore, to shorten the total length of the units, an 'excisional-expression' structure was adopted for the target unit. Although a typical target unit for conditional expression possesses (in order) the potent promoter, *lox*P, a stuffer sequence, a second *lox*P, cDNA and polyadenylation sequences (poly(A)), the excisional-expression unit lacks a stuffer sequence and instead consists of (in order) the right *lox*P, dsRed cDNA, poly(A), EF1α promoter and the left *lox*P (Figure 1, Target unit on AxLR16EL-AC). Notably, the dsRed cDNA is located not downstream, but 'upstream' of the EF1α promoter and, therefore, dsRed expression is turned off in the initial structure because AFP promoter does not function in non-hepatocarcinoma cells. However, once the AdV infects a hepatocarcinoma cell, AFP promoter is turned on and Cre enzyme is produced. Consequently, the expression unit of dsRed—EF1α promoter with one *lox*P is 'excised' as a circular molecule (Figure 1, middle), and the dsRed cDNA is now located downstream of the EF1α promoter, turning its expression on. At the same time, an AdV genome with one *lox*P is produced (Figure 1, lower, AxL-AC).

To minimize the genome size of the double-unit AdV: (i) a 0.55-kb section of the E3 region was deleted (see 'Discussion' section). In addition (ii) the EF1α promoter was shortened from an original length of 2.1 kb to lengths of 1.6 and 1.4 kb (named 16EF and 14EF, respectively). Unexpectedly, both the 16EF and 14EF promoters showed higher activity levels than the original EF1α promoter (Figure 2). As well; (iii) the 0.6-kb rabbit β-globin poly(A) sequence was truncated to 0.3 kb up to *Nde*I site. In addition to the size limitation, the double-unit AdV possesses several features that enable a very strict specificity (see Discussion section). As an improvement, the poly(A) sequence of 137 nt derived from the SV40 early region (*Hpa*I-*Bam*HI) was added in front of the dsRed cDNA plus the right *lox*P on the target unit (Figure 1, upper) based on the results of the following experiments. We constructed three AdVs containing the *lac*Z DNA tagged with the nuclear localization signal [NLacZ (3)] and their structures are shown in Figure 3a. CV1 cells were infected with each of these AdVs at multiplicity of infection (MOI) of 50 and, three days later, the *lac*Z expression of the infected cells was detected with X-gal staining. When cells were infected with AxNZ containing promoterless NLacZ (Figure 3a, top), weak but significant background expression was observed in most of the cells (Figure 3b, lower left); such expression was not observed in mock-infected cells (Figure 3b, upper left). When cells were infected with AxLNZCAL containing an excisional expression unit lacking the poly(A) in front of the NLacZ plus *lox*P (Figure 3a, middle), significant expression was observed (Figure 3b, upper right) and the expression level was much higher than that using AxNZ (lower left). We speculate from these results that a weak cryptic promoter may present upstream of the NLacZ and be activated by the enhancer of CAG promoter downstream of the NLacZ. Nevertheless, using AxALNLZCAL containing the excisional expression unit possessing poly(A) in front of NLacZ DNA plus *lox*P (Figure 3a, bottom), the background expression was almost disappeared (Figure 3b, lower right). The result showed that the inserted poly(A) sequence effectively reduced the background expression. The results were confirmed in the transfection experiments using the cosmids containing the full-length AdV genome (data not shown). Finally, we attempted to construct two AdVs, AxLR16EL-AC (104.9% of wild-type adenovirus genome) and AxLR14EL-AC (104.4%) containing the 16EF and 14EF promoters, respectively. The genome sizes of both AdVs were under the size limit.

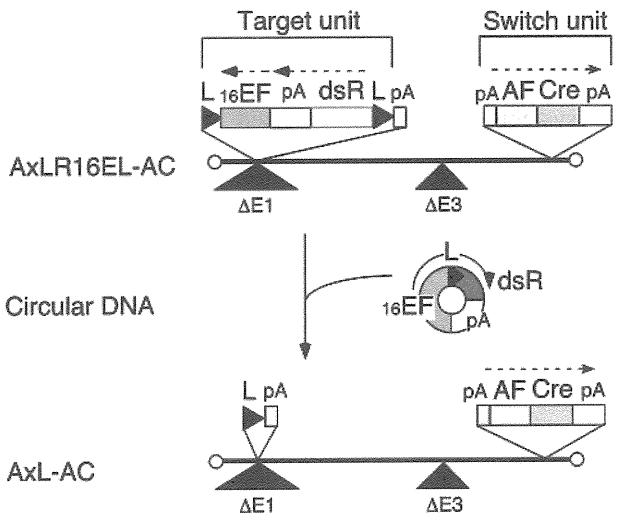

Figure 1. Structure of double-unit AdV and generation of expressing circular DNA. L, *lox*P; 16EF, shortened EF1α promoter; pA, poly(A) sequence; dsR, dsRed cDNA; AF, AFP promoter; Cre, nuclear localization signal-tagged Cre cDNA.

Leak expression of Cre both in *E. coli* and in 293 cells hampers the preparation of double-unit AdVs

Unexpectedly, during the construction of cosmids containing either AxLR16EL-AC or AxLR14EL-AC DNA (Figure 4a, dnCreRY –), we observed the co-generation of cosmids lacking the sequences between the two *lox*Ps (Figure 4b). The 2.5- and 2.7-kb bands (Figure 4c, lane 3) showed the presence of both cosmid DNA containing the AxL-AC genome and the excised circular DNA molecule, respectively. Judging from the intensities of the bands, the AxL-AC DNA accounted for ~15–20% of the midi-preparation (23) of *E. coli*. Thus, Cre must be expressed during cosmid preparation in *E. coli* DH5α despite the absence of an obvious *E. coli* promoter in the cosmid: the ampicillin promoter was present, but in the opposite orientation and ~20 kb away. Although the AxL-AC cosmid DNA was detected only faintly in the DNA of

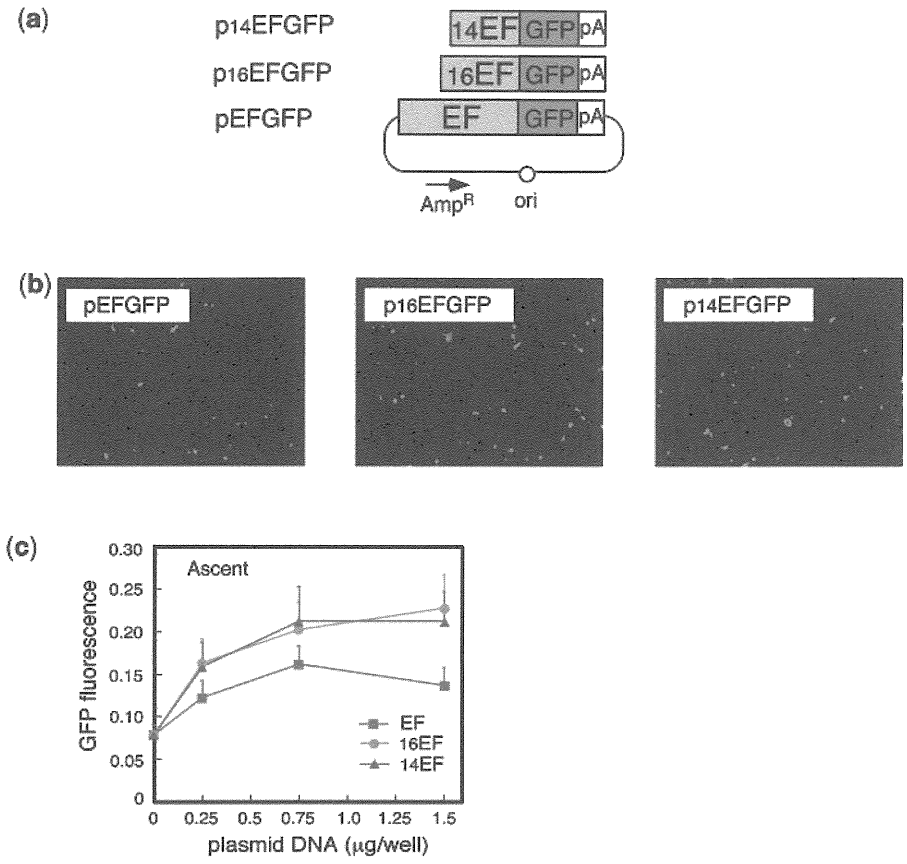

Figure 2. Expression of truncated EF1α promoter. (**a**) Structure of the plasmids expressing GFP under truncated EF1α promoter. The original EF1α promoter is 2.1-kb long. The 5′-end of 16EF was the *Ppu*MI site and that of 14EF was the *Blp*I site. (**b**) Images obtained using fluorescent microscopy. (**c**) Fluorescence measured using a fluoroscan plate reader. Vertical axis showed florescence in arbitrary unit; $n = 4$.

the mini-preparation (lane 2), it appeared to accumulate over time.

Furthermore, after the transfection of the cosmid DNA containing AxLR16EL-AC into 293 cells, all 12 of the viral clones that were generated were not the target virus, but apparently an AxL-AC virus. And three out of 18 viral clones derived from AxLR14EL-AC-containing cosmid DNA were mixtures of AxLR14EL-AC and AxL-AC viruses, while the other 15 clones were apparently pure AxL-AC virus (data not shown). These results showed that AFP promoter, which is thought to be inactive in non-hepatocellular 293 cells, certainly produced Cre in an amount sufficient to recombine the *lox*Ps on the AdV genome. This result probably occurred because even if the AFP promoter was strictly regulated, the AdV genome containing the switch unit of AFP promoter and Cre was amplified for 100 000 copies in one 293 cell and, consequently, an effective amount of Cre would be produced. Therefore, because of the leakage of Cre expression in both *E. coli* and 293 cells, double-unit vectors could not be prepared using conventional methods.

Successful suppression of leak expression of Cre using a dominant-negative of Cre and shRNA against Cre

To suppress the leak expression of Cre in *E. coli*, several dominant-negatives of Cre containing two amino acid mutations at the active center of Cre enzyme were constructed; dnCreRY, the dominant-negative that most efficiently suppressed Cre activity among those tested in co-transfection assays with a target plasmid, was then selected. Next, we constructed an expression unit producing dnCreRY under the control of the *trc* promoter of a *lac* operon system, and this unit was inserted into the cosmids containing AxLR16EL-AC and AxLR14EL-AC DNAs (Figure 4a, dnCreRY +). In the midi-preparation of this AxLR16EL-AC cosmid, neither the recombined AxL-AC-derived band nor the excised circular DNA molecule was detected with IPTG induction (Figure 4c, lane 7), showing that the production of dnCreRY successfully suppressed the leak expression of Cre in *E. coli*. Interestingly, since an apparent complete suppression was also observed without IPTG induction (lane 6), dnCreRY produced by the basal activity of the *trc* promoter was sufficient to suppress the leak expression of Cre effectively. Therefore, the problem of the leak expression of Cre in *E. coli* was solved.

To suppress the leak expression of Cre during AdV preparation in 293 cells, a plasmid expressing dnCreRY and a puromycin-resistant (PurR) gene (Figure 5a, upper) was transfected into 293 cells and the cell line 293dnCreRY8 was established; this cell line suppressed Cre activity the most efficiently. Virus clones were

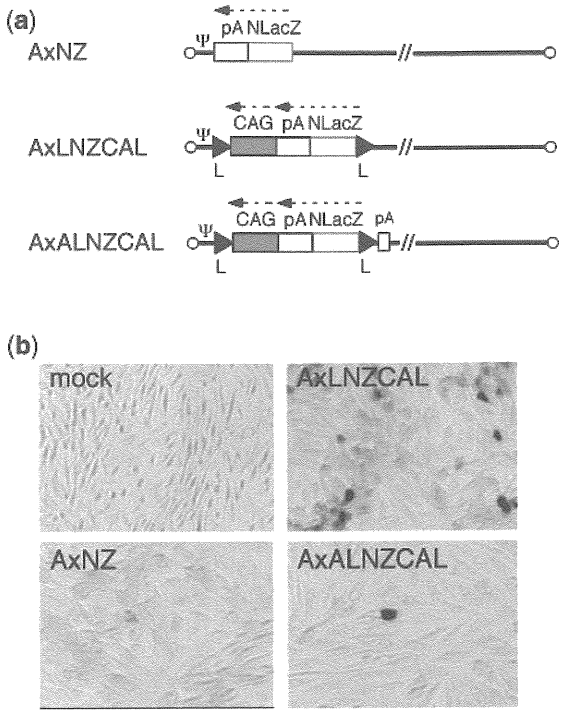

Figure 3. Suppression of the background expression by adding poly(A) sequence in front of *lac*Z DNA. (**a**) Structure of AdVs. (top) AxNZ contains the promoterless *lac*Z DNA; (middle) AxLNZCAL contains the excisional expression unit lacking poly(A) sequence in front of *lac*Z DNA plus right *lox*P; (bottom) AxALNZCAL contains that unit possessing poly(A) sequence in front of *lac*Z DNA plus right *lox*P. NlacZ, *lac*Z DNA tagged with NLS; Ψ, adenovirus packaging sequences; CAG, CAG promoter. The other representations are the same as in Figure 1. (**b**) Reduction of the 'background' expression observed using the promoterless *lac*Z DNA caused by addition of the poly(A) sequence. The infected CV1 cells were stained by X-gal. Very few dark-stained cells were observed in panels AxNZ (lower left) and AxALZCAL (lower right); the origin of these cells were unknown but possibly similar to those observed in Figure 7b and e.

obtained by transfecting linearized AxLR16EL-AC DNA, and the digestion of the viral genome with *Bmg*BI yielded a 1.8-kb band from an intact AxLR16EL-AC virus and a 1.4-kb band from a processed AxL-AC virus (Figure 5c). The 293dnCreRY8 cells did not produce pure AxLR16EL-AC virus, but instead produced mixtures of AxLR16EL-AC and AxL-AC (Figure 5a, lower, lanes 1, 3, 4 and 6) or mostly AxL-AC (lanes 2 and 5). Therefore, the suppression of Cre activity in the 293dnCreRY8 cells was not complete.

Meanwhile, several sh RNAs against Cre were constructed and screened, and shCreD was identified. Then, a plasmid expressing shCreD and PurR (Figure 5b, upper) was transfected into 293 cells, and the cell line 293shCreD13 was established. Unlike 293dnCreRY8, 293shCreD13 yielded mostly viral stocks of apparently pure AxLR16EL-AC virus (Figure 5b, lower, lanes 2, 3, 4 and 5), though some stocks were mixtures of both viruses (lanes 1 and 6). The AxLR16EL-AC virus in the apparently pure stocks was amplified in 293shCreD13 cells. To examine the 'leaky' expression level of Cre during the production of the double-unit vector in 293shCreD13 cells, an aliquot of AxLR16EL-AC viral stock was used to infect 293shCreD13 cells; then, to detect the viral genome, the total cell DNA was digested with *Bmg*BI. The 1.4-kb band produced by Cre recombination was not detected up to and including the third stock (data not shown) but, when the fourth stock purified using CsCl ultracentrifugation was examined, observed were the bands showing that the ratio of intact AxLR16EL-AC and 'leaked' AxL-AC was ~10:1 (Figure 5b, lower right). Of note, contamination with the AxL-AC virus does not cause any non-specific expression because Cre-processed AxL-AC virus does not contain an expression unit (Figure 1, bottom). An important point is that to prepare a double-unit AdV, the selection of an apparently

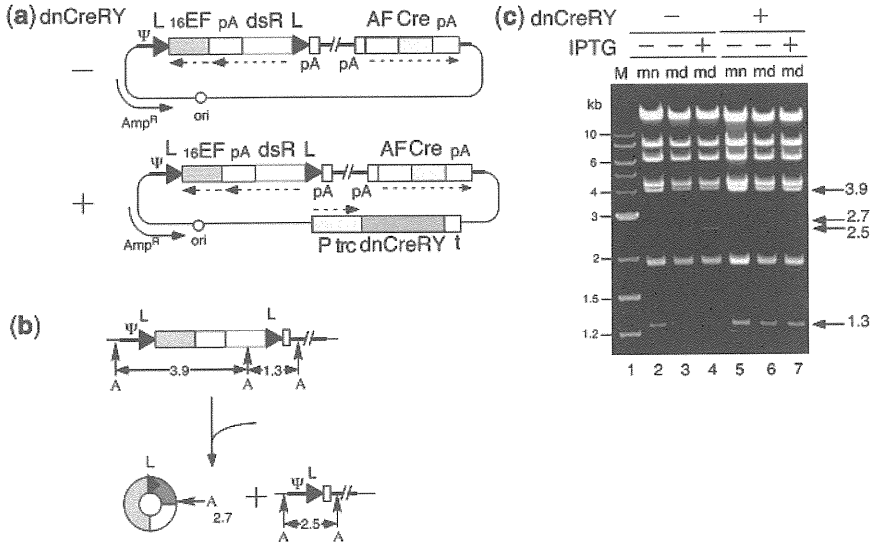

Figure 4. Leak expression of Cre in *E. coli*. Representations are the same as in Figure 1 unless otherwise stated. (**a**) Structure of cosmid generating double-unit AdV and expressing dnCreRY. Ψ, adenovirus packaging sequences; P trc, trc promoter; t, terminator. (**b**) Generation of Cre-processed molecules. A, *Ahd*I site. (**c**) Detection of Cre-processed molecules. M, 1-kb ladder marker; mn, mini-preparation; md; midi-preparation. The bands of 2.7 and 2.5 kb represent the generated circular DNA and Cre-processed DNA, respectively.

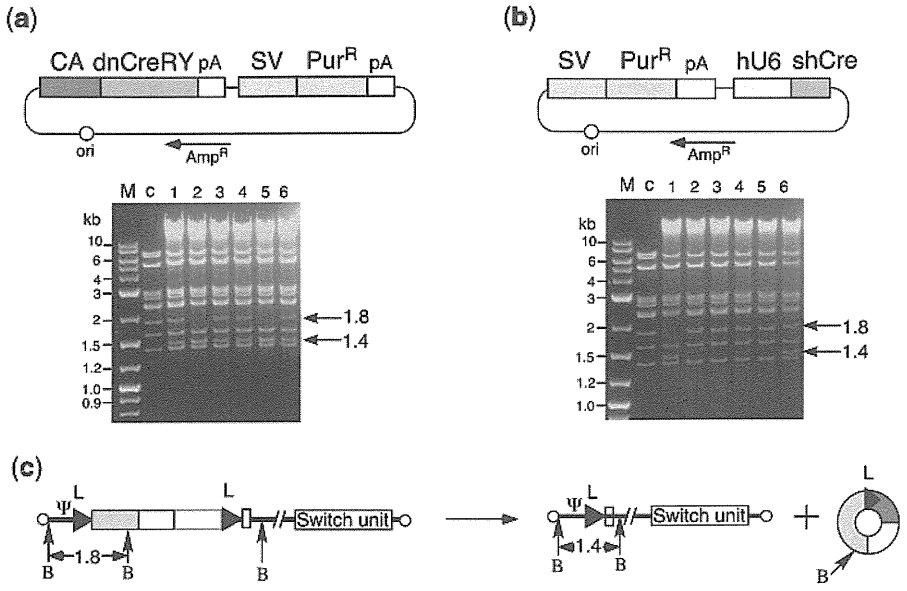

Figure 5. Establishment of 293 cell lines suppressing Cre activity. (**a**) Structure of plasmids expressing dnCreRY (upper) and DNA restriction pattern of double-unit viral clones produced in 293dnCreRY8 cells (lower). CA, CAG promoter; SV, SV40 early promoter; Pur^R, puromycin-resistant gene. The other representations are the same as in Figure 1. M, 1-kb ladder marker; c, restriction pattern of AxLR16EL-AC-containing cosmid DNA, presenting as a 1.8-kb band. (**b**) Structure of plasmids expressing shCre (upper) and DNA-restriction pattern of double-unit virus DNA of double-unit viral clones produced in 293shCreD13 cells (lower). hU6, human U6 promoter. P, purified/fourth stock was infected. The other representations are the same as in (a). (**c**) Generation of AxL-AC. B, *Bmg*BI site. The other representations are the same as in Figure 1. The presence or absence of circular 2.7-kb DNA was not clear in the gels of (a) and (b) because of the viral-derived bands of 2.9, 2.7 and 2.6 kb, but the circular DNA was hardly detected in the other experiment (data not shown). This result suggests that the production of the circular molecule occurs just after transfection and is consistent with the result that AxLR16EL-AC was stable up to the fourth stock.

Table 2. The viral titers of double-unit virus and the sprit viruses

Viruses[a]	Cells	Titers[b] ($TCID_{50}$)
AxLR16EL-AC	293shCreD13	1.1×10^{10}
AxLR16EL	Normal 293	4.7×10^{11}
Ax-AC	Normal 293	7.6×10^{10}

[a]The structure of AxLR16EL-AC is shown in Figure 1. The structures of split viruses, AxLR16EL and Ax-AC were shown in Figure 7a.
[b]Forth, purified viral stocks used in all experiments in this work.

pure first virus stock lacking AxL-AC as shown in Figure 5b, lower left, may be essential (see 'Discussion' section).

The 293shCreD13 cells grew well, similar to normal 293 cells, and the double-unit viruses were apparently able to proliferate in 293shCreD13 cells as well as normal E1-deficient AdV in 293 cells. Table 2 shows the titers of the double-unit virus AxLR16EL-AC produced in 293shCreD13 cells and of the split viruses shown in Figure 7a produced in normal 293 cells, all of which were used in this work. The titer of the double-unit virus was sufficiently high, though it was lower than those of the split viruses. One possible reason may be that the genome size of the former is near the upper limit. The AxLR14EL-AC virus was similarly prepared, and AxL-AC virus contamination was not detected in the third stock (data not shown).

The third viral stocks of double-unit virus without CsCl purification produced low but not negligible levels of non-specific dsRed expression when infected in HeLa cells (data not shown). Importantly, however, a viral preparation that was purified using a CsCl step gradient (22) did not produce any non-specific expression (see 'Discussion' section). Therefore, double-unit AdVs prepared in 293shCreD13 and purified using a CsCl step-gradient enabled the creation of viral stocks with a very strict specificity.

High-efficiency and very strict expression using double-unit AdV

The AxLR16EL-AC virus (at MOI of 5) was used to infect various cell types including HeLa (derived from non-liver carcinoma), SK-Hep1 (hepatocarcinoma-derived, non-producer of AFP), HuH-7 and HepG2 (hepatocarcinoma-derived producer of AFP). On day 3, high-level expressions of dsRed were observed in the infected HuH-7 and HepG2 cells (Figure 6h and k). Fluorescence-activated cell sorter (FACS) analyses showed that ~86 and 92% of these cells expressed detectable levels of dsRed, respectively (Figure 6i and l). In contrast, only one or two cells in a field of HeLa or SK-Hep1 cells expressed detectable levels of dsRed (Figure 6b and e), showing that the expression specificity of this vector was very strict. The FACS analyses confirmed that only 0.7 and 0.5% of the respective cells expressed detectable dsRed (Figure 6c and f). The results of dose-dependent experiments for all four cell lines confirmed the specificity of expression (Supplementary Figure S1).

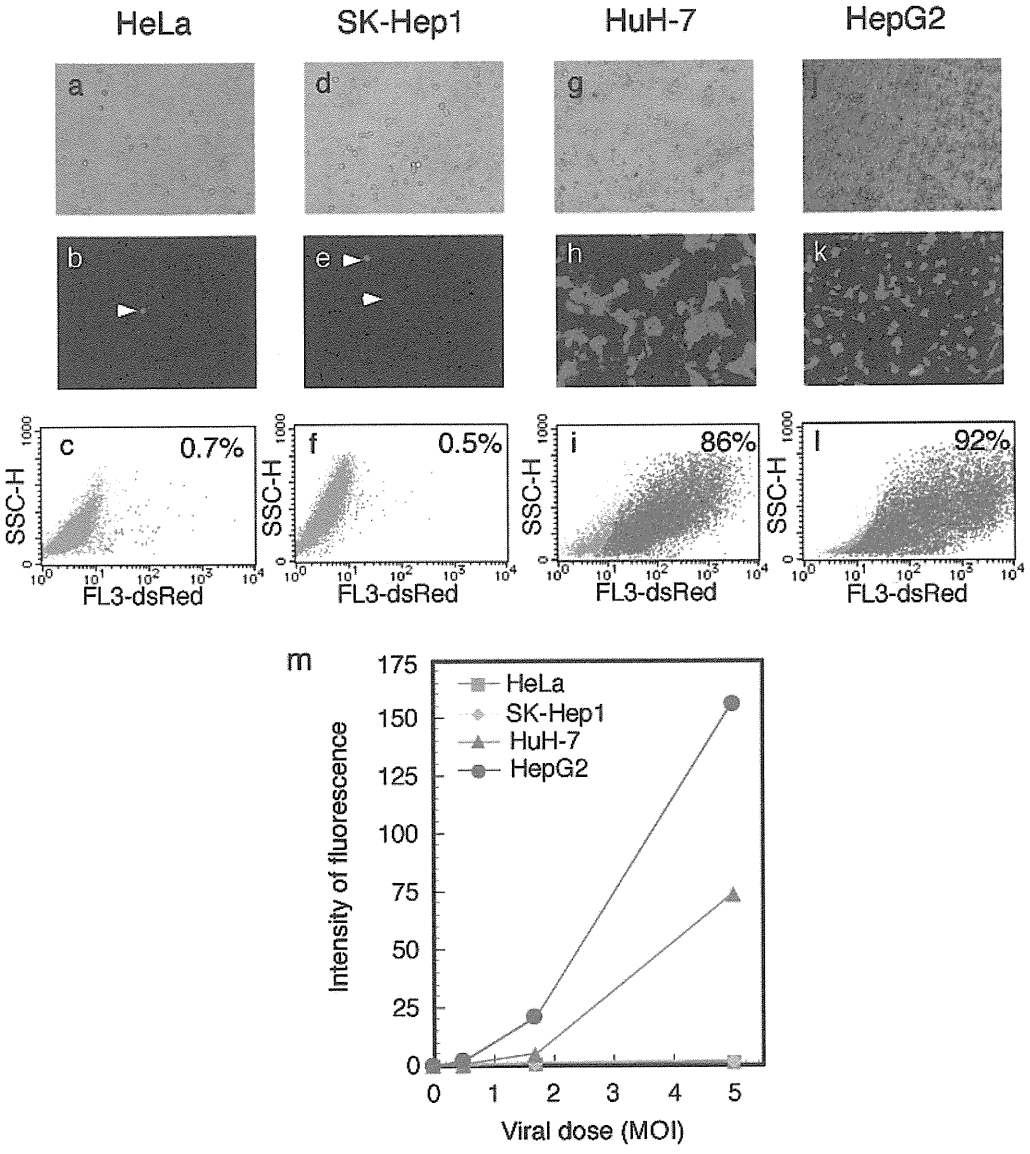

Figure 6. Specific and high-level expression of dsRed by AFP promoter using double-unit virus. Cells were infected with AxLR16EL-AC at MOI 5. (**a–c**) HeLa; (**d–f**) SK Hep-1; (**g–i**) HuH-7; (j, k and l) HepG2. (a, d, g and j) Phase-contrast microscopic views. (b, e, h and k) Images obtained using fluorescent microscopy. The arrow heads show exceptional cells with non-specific fluorescence. (c, f, i and l) FACS analysis of dsRed-expressing cells. SSC-H, side scattered light, high flow rate. (m) Dose responses of dsRed expression in the infected cells.

The dsRed expression was quantified using FACS by measuring the total sum of all cell fluorescence. The results showed that the ratio of the expressed mean fluorescence among the HeLa:SK-Hep1:HUH-7:HepG2 at MOI 5 in Figure 6c, f, i and l was 0.7:1:36.6:77.4, showing that the level of 'leaked' expression in the total cell population of AFP-negative cells compared with that in the AFP-positive cells was ~40 to 80 times less. The results of dose-dependent experiments are shown in Figure 6m. These results showed a very high expression and a strict specificity of this vector. Parallel to these FACS experiments, the transduction efficiency of the AdVs was measured by examining aliquots of all the four cell lines using real-time PCR as described in 'Materials and methods' section. The results indicated that the ratio of transduction efficiencies among HeLa, SK-Hep1, HuH-7 and HepG2 were 1.3:1:1.2:7.6, showing that the number of transduced AdV genomes present was almost the same for the first three cells. Therefore, these results confirmed very strict specificity of this vector for HeLa and SK-Hep1 cells. Meanwhile, HepG2 cells reproductively showed exceptionally high transduction efficiency. This seemed to be associated with the result that HepG2 showed much higher expression levels than HuH-7 cells (Figure 6m, at MOIs 1.7 and 5). Therefore, the very high expression level of HepG2 was partly explained by its exceptionally high transduction efficiency.

To examine the specificity of the double-unit vector, total RNA and DNA were extracted from AxLR16EL-AC-infected SK-Hep1 (AFP-negative) and HuH-7 (AFP-positive) cells. The amounts of expressed